The Peptidomimetic, 1-Adamantyl-Substituted, and Flex-Het Classes of Retinoid-Derived Molecules: Their Structure-Activity Relationships and Retinoid Receptor-Independent Anticancer Activities

M.I. Dawson* and J.A. Fontana

Sanford-Burnham Medical Research Institute, 10901 North Torrey Pines Road, La Jolla, CA 92037, USA, and John D. Dingell Veterans Administration Medical Center and Wayne State University School of Medicine, 4646 John R Street, Detroit, MI 48201, USA

Abstract: Increasing evidence demonstrates that three classes of molecules originally derived from all-trans-retinoic acid and its synthetic analogues, which function by interacting with the retinoid nuclear receptors, exert their anticancer activities through alternative signaling pathways. Thus, the methylene-linked analogues (4-HBR, 4-HPRCG, and 4-HBRCG) of *N*-(4-hydroxyphenyl) retinamide (4-HPR) and its *O*-glucuronide metabolite (4-HPROG), the cinnamic acid analogues (3-Cl-AHPC and AHPC/ST1926) of 6-[3´-(1-adamantyl)-4´-hydroxyphenyl)]-2-naphthalenecarboxylic acid, and *N*-(2,3-dihydro-2,2,4,4-tetramethyl-6-benzothiopyranyl),*N*´-(4-nitrophenyl)thiourea (SHetA2) induce cancer cell-cycle arrest and apoptosis mediated most likely through mitochondrial and/or endoplasmic reticulum stress responses. Structure–activity relationships and potential for clinical translation as anticancer therapeutics are presented.

Keywords: 3-Cl-AHPC, 4-HPR, AHPC, AHPN, apoptosis, cell-cycle arrest, retinoid-related molecule, SHetA2, ST1926.

INTRODUCTION

With the exception of retinoic acid receptor (RAR)-selective all-trans-retinoic acid (ATRA in Fig. (**1**)) currently used for the treatment of acute promyelocytic leukemia (APL), two RAR subtype α-selective retinoids undergoing or slated for the clinical trials as a second-line of defense against APL, and retinoid X receptor (RXR)-selective bexarotene used for treatment of cutaneous T-cell lymphoma, retinoids have not achieved their initial promise as anticancer therapeutics. The enormous synthetic effort in this area, however, has produced several potentially exciting new retinoid-derived molecules that are currently being evaluated for their anticancer potential. Most interesting are the findings that these retinoid-derived molecules exert their cancer cell growth inhibitory and apoptosis-inducing activities through signaling pathways that are independent of interaction with the retinoid nuclear receptors (RARs and RXRs). Among these compounds are (i) the peptidomimetic analogues of *N*-(4-hydroxyphenyl) trans-retinamide (4-HPR) and its *O*-glucuronide metabolite (4-HPROG), in which the amide NH and glucuronide O atoms have been replaced by methylene (CH_2) groups; (ii) 1-adamantyl-substituted phenols derived from the anti-acne drug and RARβ/γ-selective retinoid adapalene (6-[3´-(1-adamantyl)-4´-methoxyoxyphenyl]-2-naphthalalenecarboxylic acid); and (iii) *N*-(heterocyclic),*N*´-(4-substituted phenyl)ureas and thioureas derived from the RAR-selective retinoid (*E*)-4-[2-(5,6,7,8-tetrahydro-5,5,8,8-tetramethyl-2-naphthyl)propenyl]benzoic acid (TTNPB). These structures are shown in Fig. (**1**). The sections below describe how these compounds evolved from the classical retinoids that function by interacting with the retinoid nuclear receptors, their syntheses, structure–activity relationships, and potential mechanisms of action. Interestingly, the three compound classes exert similar effects on cancer cells to induce their apoptosis. However, their initial targets and downstream signaling events remain to be fully identified.

*Address correspondence to this author at the Sanford-Burnham Medical Research Institute, 10901 North Torrey Pines Road, La Jolla, CA 92037, USA; Tel: 858-646-3165; Fax: 858-646-3197;
E-mail: mdawson@burnham.org

N-(4-HYDROXYPHENYL) RETINAMIDE, ITS GLUCURONIDE METABOLITE, AND THEIR PEPTIDOMIMETIC ANALOGUES

Overview

Results from clinical trials using *N*-(4-hydroxyphenyl) retinamide (4-HPR, fenretinide, **1** in Fig. **1** and Table **1**) for prevention of the appearance of second primary tumors in the contrateral breast of women at risk for breast cancer reappearance have not been statistically significant overall, although significant latency and regression had previously been observed in rat models of 7,12-dimethylbenz[*a*] anthracene (DMBA)-induced mammary cancer prevention and treatment [1-5]. Dr. Michael B. Sporn and colleagues (National Cancer Institute, Bethesda, MD) had discovered that dietary glucurate (the salt of D-glucuronic acid) synergized with 4-HPR to inhibit the DMBA-induced rat mammary tumors [6]. These results led Dr. Robert W. Curley, Jr. and colleagues (Ohio State University School of Pharmacy, Columbus, OH) to speculate that after glucurate had equilibrated to the β-glucuronidase inhibitor D-glucuro-1,4-lactone in the stomach, plasma levels of the 4-HPR metabolite 4-HPR-*O*-glucuronide (4-HPROG in Fig. **1** and Table **3**) would have increased. The body employs β-glucuronidation to detoxify and solubilize unwanted compounds to permit their excretion through the kidney or intestine. The observa-

1389-5575/10 $55.00+.00 © 2010 Bentham Science Publishers Ltd.

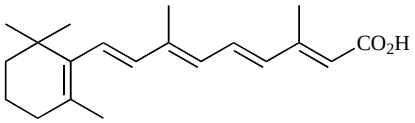

All-trans-retinoic acid (ATRA)

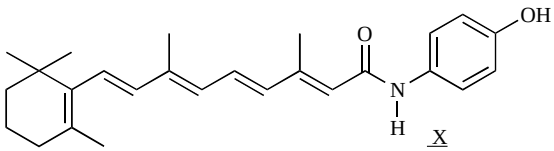

	X
N-(4-Hydroxyphenyl) retinamide (4-HPR)	NH
4-(Retinoylmethyl)phenol (4-HBR)	CH_2

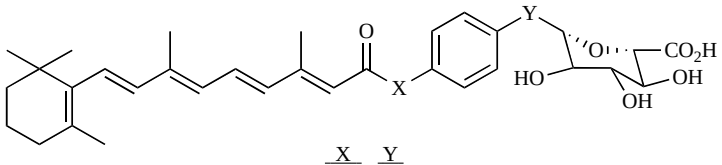

	X	Y
4-HPROG	NH	O
4-HPRCG	NH	CH_2
4-HBRCG	CH_2	CH_2

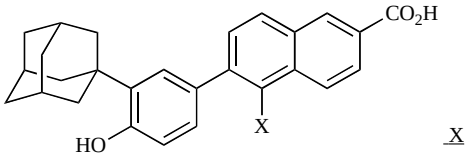

	X
6-[3′-(1-Adamantyl)-4′-hydroxyphenyl)-2-naphthalenecarboxylic acid (AHPN / CD437)	H
5-Cl-AHPN (MM001)	Cl

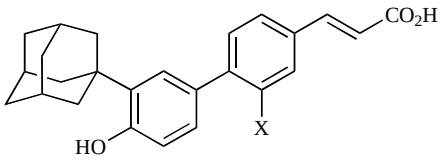

	X
(*E*)-4-[3′-(1-Adamantyl)-4′-hydroxyphenyl)cinnamic acid (AHPC / SR11298 / ST1926)	H
3-Cl-AHPC (MM002)	Cl

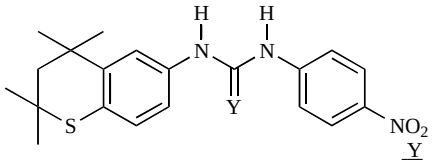

	Y
N-(2,3-Dihydro-2,2,4,4-tetramethyl),-*N*′-(4-nitrophenyl)lthiourea (SHetA2)	S
N-(2,3-Dihydro-2,2,4,4-tetramethyl),-*N*′-(4-nitrophenyl)urea (SHetC2)	O

Fig. (1). Structures of all-trans-retinoic acid (ATRA) and retinoid-related or derived molecules such as *N*-(4-hydroxyphenyl) retinamide (4-HPR), its *O*-glucuronide metabolite (4-HPROG), their peptidomimetic analogues (4-HBR, 4-HPRCG, and 4-HBRCG); adamantyl-substituted retinoid-related molecules such as 6-[3′-(1-adamantyl)-4′-hydroxyphenyl]-2-naphthalenecarboxylic acid (AHPN / CD427), its 5′-chloro analogue (5-Cl-AHPN / MM001), (*E*)-4-[3′-(1-adamantyl)-4′-hydroxyphenyl]cinnamic acid (AHPC / SR11298 / ST1926), and its 3-chloro analogue (3-Cl-AHPC / MM002); and the flexible heteroaromatic retinoids *N*-(2,3-dihydro-2,2,4,4-tetramethyl-6-dihydrobenzothiopyranyl),*N*′-(4-nitrophenyl)thiourea (SHetA2) and *N*-(2,3-dihydro-2,2,4,4-tetramethyl-6-dihydrobenzothiopyranyl),*N*′-(4-nitrophenyl) urea (SHetC2).

tions that 4-HPROG had antiproliferative activity against cultured leukemia cells and mammary tumors and a 24-h half-life on take-up by organs after intraperitoneal injection suggested that it might be inherently active. Dr. Curley improved the synthesis 4-HPROG [7], which had been reported earlier by Dawson and Hobbs [8], and then he and his colleagues showed that 4-HPROG and 4-HPR were not interconverted in MCF-7 breast cancer cells over a 24-h period to support the hypothesis that 4-HPROG was an active species and not a precursor to 4-HPR [7]. Moreover, 4-HPROG demonstrated anticancer activity in the rat mammary tumor model and was less toxic to cells in culture than 4-HPR. To further demonstrate that the glucuronide was active without being cleaved to 4-HPR or ATRA (Fig. (**1**)), the Curley group next synthesized and evaluated peptidomimetic analogues of 4-HPR and 4-HPROG in collaboration with Dr. Hussein Abou-Issa (Ohio State University) and Dr. Margaret Clagett-Dame (University of Wisconsin, Madison, WI). The hydrolyzable amido (CONH) and *O*-glycosyl bonds of 4-HPR and 4-HPROG were replaced with methylene (CH_2) groups to give 4-(all-trans-retinoylmethyl)phenol (4-HBR), 2,6-anhydro-7-deoxy-7-[4-(retinamido)phenyl]-L-glycero-L-guloheptinoic acid (4-HPRCG), and 2,6-anhydro-7-deoxy-7-[4-(retinoylmethyl)phenyl]-L-glycero-L-guloheptinoic acid (4-HBRCG), the structures of which are shown in Table **3**.

Synthesis

The syntheses of 4-HPR, 4-HPRCG, 4-HBR, and 4-HBRCG are illustrated in Scheme **1**. All-trans-retinoic acid (ATRA) was first activated as its retinoyl chloride and then allowed to react with an aniline to produce the desired retinamide or a protected analogue of 4-HPR [9]. The introduction of the glucuronide group in 4-HPRCG and 4-HBRCG has proved to be synthetically challenging as the published routes have produced only modest yields [1, 4].

Structure–Activity Relationships

In a series of substituted phenol, benzoate, and naphthol-terminated analogues, 4-HPR (**1** in Table **1**) continued to be the most potent at inhibiting the growth and inducing the

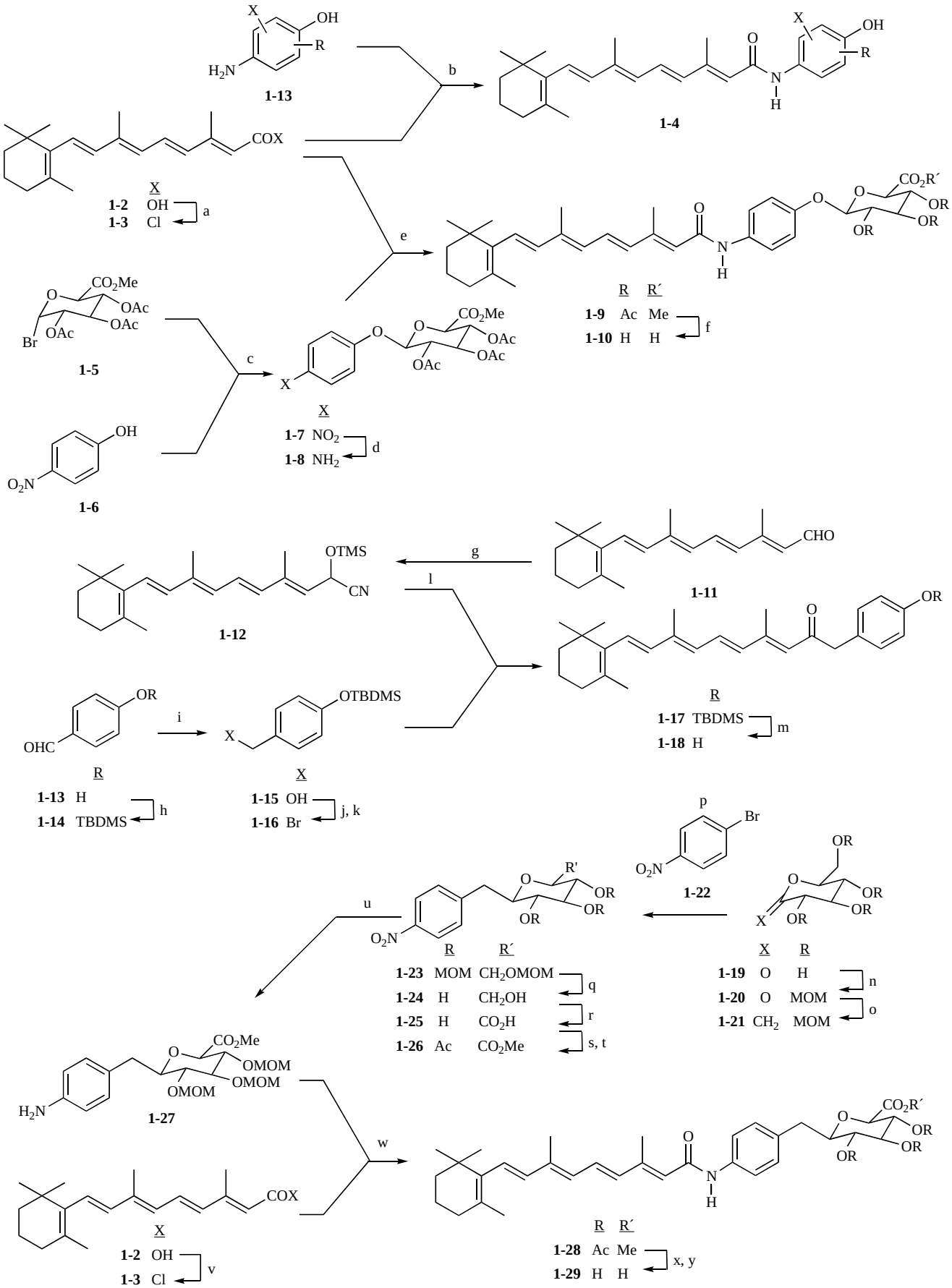
1-13
1-4
1-2 OH
1-3 Cl
a
b
e
1-5
1-6
c
1-7 NO2
1-8 NH2
d
1-9 Ac Me
1-10 H H
f
1-12
1-11
g
l
1-17 TBDMS
1-18 H
m
i
1-13 H
1-14 TBDMS
h
1-15 OH
1-16 Br
j, k
p
1-22
u
1-23 MOM CH2OMOM
1-24 H CH2OH
1-25 H CO2H
1-26 Ac CO2Me
q
r
s, t
1-19 O H
1-20 O MOM
1-21 CH2 MOM
n
o
1-27
w
1-28 Ac Me
1-29 H H
x, y
v

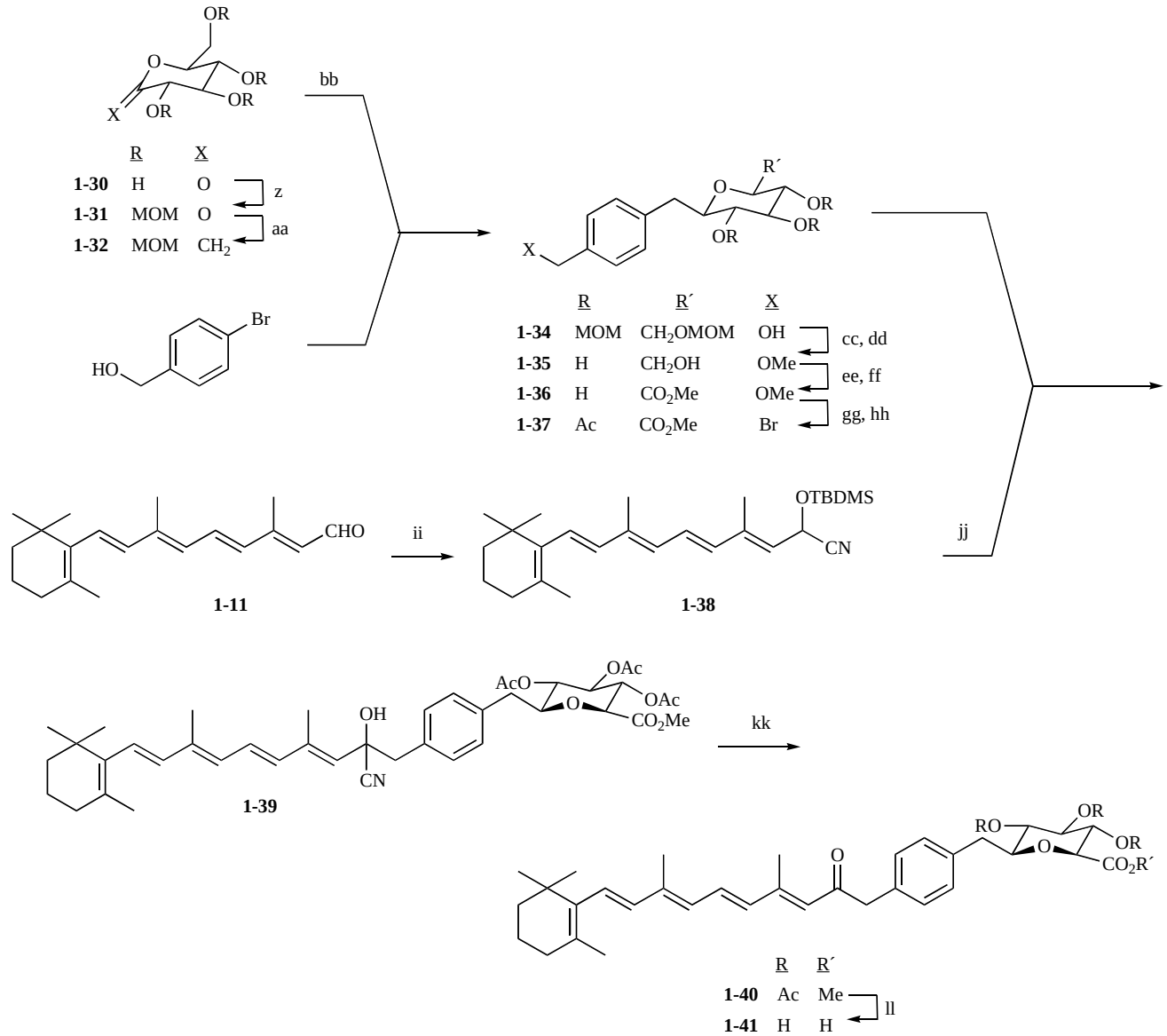

Scheme 1. (a) Resin–Ph_3P, THF, $Cl_3CC(O)CCl_3$, 0 °C [9]. (b) $ArNH_2$, pyridine, 0 °C to rt; F_4-phthalic anhydride; Amberlite A-21 amine ion exchange resin (20–94% for steps a and b) [9]. (c) Ag_2O [145]. (d) H_2 [145]. (e) (73%) [8, 145]. (f) Saponification; 1 N HCl (92%) [8, 145]. (g) Me_3SiCN, Et_3N, CH_2Cl_2 (100%) [3]. (h) NaH, THF; *t*-$BuMe_2SiCl$ (100%) [3]. (i) $NaBH_4$, EtOH (94%) [3]. (j) $(CF_3CO_2)_2O$, THF (95%) [3]. (k) LiBr, THF (73%) [3]. (l) $Na_2(Me_3SiN)_2$, THF; **1-16**, THF [3]. (m) $(n\text{-}Bu)_4NF$, THF/H_2O (9:1) (65% for l and m) [3]. (n) $MeOCH_2Cl$, $(i\text{-}Pr)_2MeN$, $(n\text{-}Bu)_4NI$, CH_2Cl_2 (83%) [2]. (o) (Cyclopentadiene)$_2TiMe_2$, PhMe, 70 °C (87%) [2]. (p) 9-BBN-H, THF, reflux; **1-22**, $PdCl_2(Ph_2P$-ferrocene), 3 M K_3PO_4, DMF (54%) [2]. (q) 6 N HCl, MeOH. (r) 2,2,6,6-Me_4-piperidinyloxy radical, NaOCl, KBr, $NaHCO_3$. (s) HCl(g), MeOH, 40 °C. (t) Ac_2O, 4-Me_2N-pyridine, pyridine (84% for p–t) [2]. (u) H_2, Pd(C), EtOAc (98%) [2]. (v) $SOCl_2$, pyridine. (w) **1-3** and **1-27** (86% for v and w) [2]. (x) K_2CO_3, MeOH. (y) 5 N KOH, MeOH; H_3O^+ (86% for x and y) [2]. (z) $MeOCH_2Cl$, $(i\text{-}Pr)_2NEt$, $(n\text{-}Bu)_4NI$, CH_2Cl_2 (83%) [4]. (aa) (Cyclopentadiene)$_2Ti(Me)_2$, PhMe, 70 °C (87%) [4]. (bb) 9-BBN-H, THF, reflux; $PdCl_2(Ph_2P$-ferrocene), 3 M K_3PO_4, DMF (67%). (cc) NaH, THF; MeI (90%). (dd) 6 N HCl, MeOH. (ee) 2,2,6,6-Me_4-piperidinyloxy radical, NaOCl, KBr, $NaHCO_3$, 0 °C [4]. (ff) MeI, DMF [4]. (gg) Ac_2O, 4-Me_2N-pyridine, pyridine (82% for dd–gg) [4]. (hh) HBr, HOAc (86%) [4]. (ii) *t*-$BuMe_2SiCN$, Et_3N, CH_2Cl_2 (78%) [4]. (jj) **1-38**, $Li(Me_3SiN)_2$, THF, −78 °C; **1-37**, THF, −78 °C (47%) [4]. (kk) $(n\text{-}Bu)_4NF$, THF (75%). (ll) K_2CO_3, MeOH, 4 °C; KOH, MeOH, 4 °C; H_3O^+ (82%) [4].

apoptosis of ATRA-sensitive MCF-7 breast cancer cells, with the exception of its *N*-(2-hydroxy-5-nitrophenyl) analogue (**24**), which had comparable activity (Table **1**) [9, 10]. However, aromatic nitro groups have generally not been incorporated into the structures of drugs because of their ability to be transformed to aryl amines and reactive species. The *N*-methyl analogue (**47**) of 4-HPR had decreased anti-cancer activity but also inhibited aromatase activity to prevent the synthesis of estrogen [9]. At 5 μM, both 4-HPR (3.5-fold increase) and *N*-Me-4-HPR (4.7-fold increase) were less potent inducers of cytochrome P450 CYP19 (aromatase) gene expression than ATRA, which induced CYP19 expression (seven-fold) in MDA-MB-231 breast cancer cells [10].

Table 1. 4-HPR Analogues and Effects on Breast Cancer Cells Including Growth Inhibition, Apoptosis, and Induction of Expression of Aromatase and Cytochrome CYP19

4-HPR series	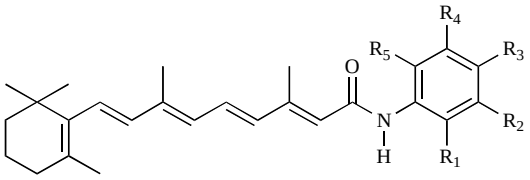					Effect on MCF-7 breast cancer cells at 10 μM after 48 h[a,b]		Aromatase activity at 5 μM for 24 h[c]	CYP19 mRNA expression in breast cancer cells at 5 μM for 24 h (%)[d]		
Cmpd No[e]	**R_1**	**R_2**	**R_3**	**R_4**	**R_5**	**Growth inhibition**	**Apoptosis (%)**	**(%)**	**SK-Br-3**	**MCF-7**	**MDA-MB-231**
1 (4-HPR)	H	H	OH	H	H	+3 +2*	100	110	99	120	190
3	CO_2H	H	H	H	H	+1	13				
7	Me	H	OH	H	H	0					
8/12	Me	H	OH	Me	H	0		106			
9/7	OH	H	Me	H	H	+2	26	195	143	187	313
10/1	OH	H	H	Me	H	0		111			
11/3	OH	H	H	CMe_3	H	0		83			
12/2	OH	H	H	H	Me	0		105			
13/11	H	OH	Me	H	H	+3	72	129			
14/9	Me	OH	H	H	H	0		106			
15	H	OH	OMe	H	H	0					
16	Cl	H	OH	H	H	0					
17	H	Cl	OH	H	H	+2	43				
18	OH	H	H	Cl	H	+2	39				
19/13	H	Cl	OH	Cl	H	0		138			
20	H	Br	OH	Br	H	0					
21	OH	Cl	Me	Cl	H	0					
22	NO_2	H	OH	H	H	0					
23/14	H	NO_2	OH	H	H	0		131			
24	OH	H	NO_2	H	H	+3	100				
25	OH	H	H	NO_2	H	+1	17				
26	OH	CO_2Me	H	H	H	0					
27/4	OH	CO_2H	H	H	H	0		86			
28/8	OH	H	CO_2Me	H	H	+1	61	99			
29/5	OH	H	CO_2H	H	H	0		112			
30	OH	H	H	H	CO_2Me	0					
31	OH	H	H	H	CO_2H	0					
32/10	H	OH	CO_2Me	H	H	0		132			
33	H	OH	CO_2H	H	H	0					
34	H	CO_2Me	OH	H	H	+1	28				

(Table 1). Contd…..

35	H	CO_2H	OH	H	H	0					
36	OH	H	H	CO_2Me	H	0					
37	OH	H	SO_2Et	H	H	0					
38	CH_2OH	H	H	H	H	ND[f]					
39	H	CH_2OH	H	H	H	+1	24				
40	H	H	NH_2	H	H	+2	35				
41	CO_2Me	H	H	H	H	ND					
42	H	H	OEt	H	H	0					
48	H	H	H	H	H	+1*					
49/16	H	H	Cl	H	H	+1*		89			
50/15 (4-MPR)	H	H	OMe	H	H	+1*	6	112			
51/17	H	H	Me	H	H	0*		128			
52/18	H	Cl	Cl	H	H	+1*		91			
53	H	H	NMe_3^+	H	H	0					
_/16	OH	H	SO_2H	H	H	0		97			
47/19	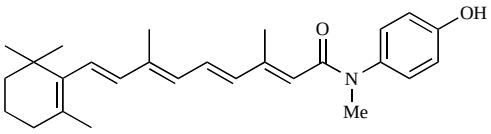					+1		33	88	65	146
Naphthol series	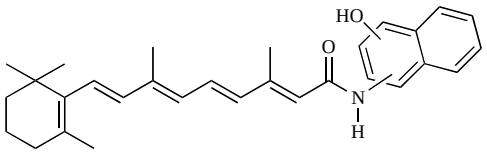										
Cmpd No[e]	**Retinoyl-NH position**		**OH position**								
43	1		2			0					
44	1		4			0					
45	1		5			0					
46/20	2		3			0		173	165	160	171
Control									100	100	100
ATRA	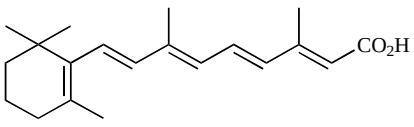							190	166	122	638

Taken from Ref. [9, 10].

[a]MCF-7 breast cancer cell growth inhibition was evaluated after 48-h treatment with 10 μM compound except for 5.9 μM **30**, 3.9 μM **31**, 6.6 μM **32**, and 7.4 μM **42** [9]. +3, ≥ 100% growth inhibitory activity of 4-HPR; +2, ≥ 50% activity; +1, ≥ 25% activity; 0, equivalent to vehicle [9]. Data labeled with an asterisk was obtained in a separate expriment [9].

[b]MCF-7 cell apoptosis was determined after 48-h treatment with 10 μM compound [10].

[c]Aromatase was measured by loss of tritium from [1β-^{3}H]androst-4-ene-3,17-dione after treatment of SK-BR-3 breast cancer cells with 5 μM retinoid for 24 h [10].

[d]Expression of CYP19 mRNA after 24-h treatment with 5 μM compound relative to DMSO control (100%) was determined by RT-PCR [10].

[e]First compound number refers to Ref. [9]; second number refers to Ref. [10].

[f]ND, not determined.

Das and coworkers also synthesized a series of substituted 4-HPR analogues (Table **2**) and evaluated them against rhabdoid cancer, a fatal cancer of children [11]. Introduction of an ortho halogen enhanced activity in the 3-iodo-4-hydroxyphenyl analogue (**5j** in Table **2**), which had the lowest IC_{50} value (3 μM) compared to 4-HPR (9 or 19 μM) in inhibiting the growth of MON ($INI1^{-/-}$) rhabdoid cancer cells in culture. However, the light and thermal instability of the ortho-iodophenol group would be problematic for the use of **5j** as a drug.

4-HPR and 4-HBR had similar activities in reducing the volumes of DMBA-induced mammary tumors in the female rat model (Table **3**). Evaluation of plasma retinol levels indicated that, like ATRA, 4-HPR treatment resulted in the reduction of plasma retinol levels, which decreased to ≤ 30% of control levels [3]. These decreases by 4-HPR were two-fold lower than that induced by 4-HBR and, thereby, increased susceptibility to night-blindness from the reduced conversion of retinol to vision-essential retinal. Competitive binding studies with labeled ATRA indicated that 4-HPR and 4-HBR had similarly low affinities for the RAR subtypes to further suggest that the hydrolysis of 4-HPR to ATRA may have had a role in reducing plasma retinol levels [4]. The promoter of the lecithin retinol acyltransferase enzyme (LRAT) that converts retinol to retinyl esters for liver

Table 2. Comparison of Inhibition of Rhabdoid Cancer Cell Growth by 4-HPR, 4-HPR Analogues with Phenyl Ring Substitutions, and ATRA

4-HPR series	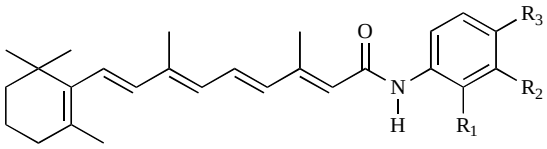			**RhC cell growth inhibition**
Cmpd No[b]	**R_1**	**R_2**	**R_3**	**IC_{50} (μM)**
5a	F	H	F	150
5b	Cl	H	Cl	>200
5c	H	H	Br	150
5d	H	H	I	NA[c]
5e	H	H	NO_2	>200
5f	H	H	OMe	NA
5g	H	H	OH	19
5h	H	F	OH	8
5i	H	Cl	OH	12.5
5j	H	I	OH	3
5k	H	NO_2	OH	NA
5l	H	H	CH_2OH	25
5m	H	H	$(CH_2)_2OH$	>50
5n	OH	H	OH	8
Control				
4-HPR	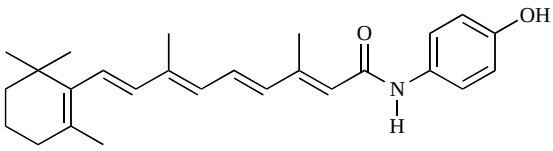			9
ATRA	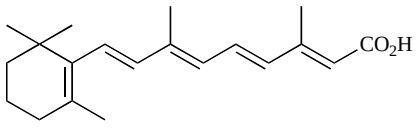			100

Taken from Ref. [11].

[a]MON ($INI1^{-/-}$) rhabdoid cancer cells (RhC) were treated with compound for 72 h before cell survival (% control) was determined using an MTS assay. IC_{50} (μM), 50% inhibition of proliferation. IC_{50} value for 4-HPR was 12 μM or 19 μM in separate experiments with **5e**, **5f**, and **5l**–**5n** and with **5h**–**5k**, respectively.

[b]Compound numbers refer to those cited in Ref. [11].

[c]NA, not active.

Table 3. Peptidomimetic Analogues of 4-HPR

4-HPR series	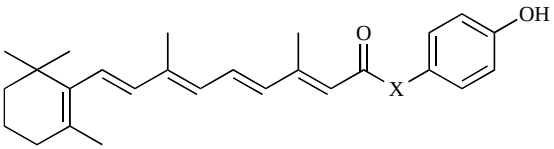										
			Mean changes in tumor volume for DMBA-initiated rats on retinoid diet compared to vehicle diet for tumor volume and those of other parameters before and retinoid treatment (%)[a]				**Expression of rat liver CYP26A1 mRNA**	**Retinoid level in plasma**	**Displacement of bound [^{3}H]ATRA from RAR (K_i, nM)[b]**		
Cmpd[c,d]	**X**		**Mammary tumor volume**	**Serum retinol**	**Serum triglycerides**	**Bone mineral content**	**Fold change induced**	**(μg/ml)**	**RARα**	**RARβ**	**RARγ**
4-HPR	NH		–49	–63	362	2	+			1,400	6,580
			–25*						>2,200*	>2,800*	>6,000*
			–77[#]	–72[#]				1.03[#]			>4,000[#]
			–33**	–63**	198**	–13**	36**	0.67**		1,500**[e]	3,500**[e]
			–42***	–62***					35%***	24%***	42%***
			–21[##]								
4-HBR	CH_2		–85[#]	–29[#]				0.05[#]			>4,000[#]
			–45***	–7***					33%***	13%***	43%***
Glycosyl series	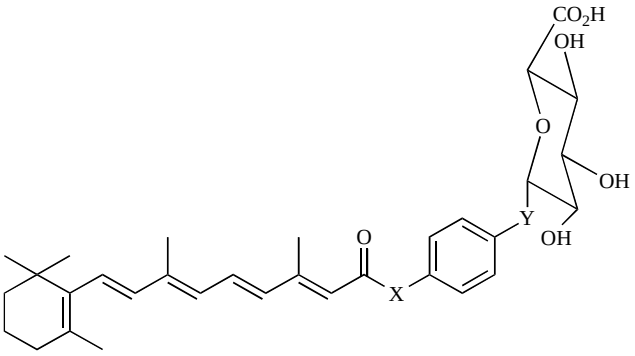										
Cmpd	**X**	**Y**									
4-HPROG	NH	O		Significant decrease							
									>2,200*	>2,800*	>6,000*
			–41[##]								
4-HPRCG	NH	CH_2	–49	–24	5	2	0			400	2,940
			–21*						>2,200*	>2,800*	ND*[f]
4-HBRCG	CH_2	CH_2	–33**	–28**	–9**	–10**	1.6**	0.10**		150**[e]	1,960**[e]

(Table 3). Contd…..

Control									
ATRA 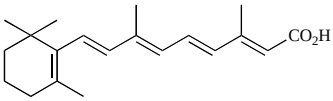	–51 –40* –74[#] –38**	–69 –67[#] –53**	545 828**	–10 –45**	+ 67**	 0.017[#] 0.30**	 0.4* ≥95%***	1.5 0.5* 5.4**	1.5 1.4* 0.7[#] 5.3** ≥96%***
Vehicle / control	86 224* 257[#] 190** 179***				1				

Taken from Ref. [1-5, 146].

[a]Female rats were initiated 4 months earlier with dimethylbenz[*a*]anthracene (DMBA) to induce palpable mammary tumors and then fed compound at 2 mmol/kg diet or vehicle alone in diet for 28 days [1]. Change (%) represents differences between tumor volumes at day 0 and day 28, or differences in levels between vehicle controls and compound-treated groups, where vehicle control levels were 0.49 ± 0.07 μg/ml for serum retinol and 38 ± 1.9 mg/dl for total triglycerides at day 10, and 0.41 ± 0.01 gm for bone mineral content as determined by scanning of the femur at day 28.

[b]Competitive binding employed murine RARβ and RXRγ and human RARγ. 4-HPR and analogues did not bind to RXRγ.

[c]4-HPR, *N*-(4-hydroxyphenyl) retinamide; 4-HBR, 4-(retinoylmethyl)phenol; 4-HPROG, *N*-(4-hydroxyphenyl) retinamide *O*-glucuronide; 4-HPRCG, *N*-(4-hydroxybenzyl) retinamide *C*-glucuronide; 4-HBRCG, 4-(retinoylmethyl)benzyl *C*-glucuronide.

[d]Nonsuperscripted data refers to Ref. [1], in which case: +, expression induced; 0, no expression induced.

Data superscripted by *, [#], **, ***, and [##], respectively, refers to: (1) Ref. [2], in which case compounds were given for 10 days at 2 mmol/kg diet to rats bearing DMBA-induced tumors, and K_i values for ATRA were 0.5 nM on RARβ and 1.4 nM on RARγ. (2) Ref. [3], in which changes in mean tumor volumes refer to those between feeding day 1 and day 21 with compounds given at 2 mmol/kg diet for 21 days starting 50 days after DMBA initiation. Retinol levels were determined at day 21 of treatment and were derived from Figure 1 of Ref. [3]; the retinol control value at day 21 was 0.26 μg/ml. (3) Ref. [4], in which compounds were fed at 2 mmol/kg diet for 22 days beginning 50 days after initiation with DMBA. Changes in plasma triglycerides and bone mineral content were compared to control values of 0.23 mg/ml and 0.449 g, respectively, which were derived from data in Fig. (4) of Ref. [4]. Fold induction values of CYP26A1 mRNA relative to that of the control at day 22 were taken from Fig. [6]. Compound levels in blood were measured at sacrifice and determined from Fig. (5A); and compound concentrations required to displace 50% of labeled ATRA were determined from Figure 5B. (4) Ref. [5], in which compounds were given at 2 mmol/kg diet for 28 days beginning at 4 months after initiation. Displacement (%) refers to amount of bound 5 nM [^{3}H]ATRA displaced from RAR subtypes by 10 μM 4-HPR and 4-HBR and 1.0 μM ATRA. (5) Ref. [146], in which compounds were given at 2 mmol/kg diet for 25 days.

[e]The text in Ref. [4] indicates that 4-HPR binding to RARβ was 3,000 times less potent than that of ATRA and to RARγ was 2,500 times less potent that of ATRA, and that the binding of 4-HBRCG to RARβ was 300 times less potent than that of ATRA and to RARγ was 1,400 times less potent than that of ATRA. Therefore, on the basis of the ATRA K_i values of 0.5 nM and 1.4 nM, the relative values for 4-HPR and 4-HBRCG were calculated and are listed above. However, the graphs in Fig. (5A) of Ref. [4] indicate that the respective IC_{50} values for binding to RARβ by ATRA, 4-HBRCG, and 4-HPR would be approximately 5.5 nM, 1,500 nM, and 20,000 nM, and the graphs in Fig. (5B) indicate that the respective IC_{50} values for binding to RARγ by ATRA, 4-HBRCG, and 4-HPR would be approximately 5.3 nM, 4,000 nM, and 25,000 nM.

[f]ND, not determined.

storage contains an retinoic acid response element (RARE) that is activated by RARα interacting with ATRA. However, 4-HPR was about half as effective as ATRA in enhancing serum triglyceride levels (2–3.6-fold and 5.5–8.4-fold, respectively) [4], a major adverse effect observed in acute promyelocytic leukemic patients undergoing ATRA therapy. The effect of 4-HBR on triglyceride levels was not reported. ATRA treatment-associated adverse events such as the reduction in bone calcification and induction of the expression of cytochrome P450 CYP26A1 were lower in rats treated with 4-HPR compared with ATRA. CYP26A1 metabolizes ATRA to less active retinoids, including 4-hydroxy-ATRA, 4-oxo-ATRA, and 18-hydroxy-ATRA, and its expression is induced by ATRA [12]. Both 4-HPRCG and 4-HBRCG had effects similar to ATRA in reducing rat mammary tumor volumes but had significantly reduced adverse effects associated with their decreases in plasma retinol levels (24% and 28% decreases, respectively) and bone calcification and their increases in serum triglycride (≤ 1%) and CYP26A1 (≤ 2%) levels [1, 4]. The binding of 4-HPRCG to RARα and RARβ was low (K_i values > 2 μM) [4] as was that of 4-HBRCG to RARγ (K_i = 2 μM), whereas that of 4-HBRCG to RARβ was more than 10-fold higher (K_i = 0.15 μM) but still < 4% of that of ATRA [2].

The D-mannose conjugate (**5c** in Table **4**) of 4-HPR was more active than the D-glucose and D-galactose conjugates (**5a** and **5b**, respectively) in inhibiting HL-60 myeloid leukemia and MCF-7 breast cancer cell proliferation; however, their activities against HT29 colon cancer cells were reversed but were the same against H460 lung cancer [13]. IC_{50} values ranged from 5–31 μM. In these comparison studies, normal cells were represented by quiescent and exponentially growing fetal lung fibroblasts and CEM lymphoblastoid cells. The therapeutic window between MCF-7 breast, HT29 colon, and H460 lung cancer and normal cell line growth inhibition was two-fold at most. In the case of HL-60 myeloid leukemia cells, higher fold differences were observed.

4-HPROG (**5**[*] in Table **4**) was three times more effective than 4-HPRCG (**8**[*]) in inhibiting MCF-7 breast cancer cell growth on the basis of their IC_{50} values, but the activity profile was reversed in the glucose congeners 4-HPRO-D-glucose (**4**[*]) and 4-HPRC-D-glucose (**7**[*]) with the former having 14-fold higher efficacy than 4-HPROG or 4-HPR [14]. None were as potent as 4-HPR. In the *in vivo* rat mammary cancer prevention model, both 4-HPRC-D-glucose and 4-HPRCG were equally effective in delaying the appearance of the first tumor to 71 days compared to the control value of

Table 4. 4-HPR Glycosyl Conjugates Inhibit Growth of Both Cancer and Normal Cells

4-HPR glycosyl series		Growth inhibition (IC_{50}, μM)[a]								Effects on mammary tumor development and growth[b,c]			RARβ binding[d]
		Cancer cells				Normal cells				Latency	Incidence	Tumors/rat	Label lost (%)
Cmpd No[e]	Structure	LeuC	BC	CC	LC	FLB stat	FLB expon	PBM	CEM	Days	% with tumors	Mean number	at 10 μM
5a/4* (4-HPRO-D-Glucose	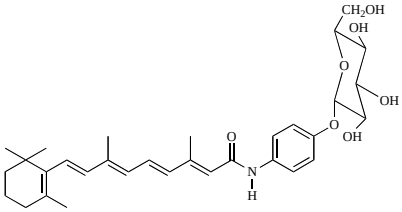	7.5	29.3 27.0*	7.5	29.3	20.0	15.5						
5b (4-HPRO-D-Galactose	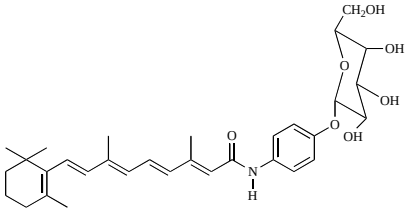	5.3	26.3	20.5	28.6	25.1	14.0						
5c (4-HPRO-D-Mannose	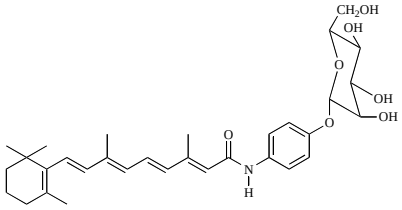	4.9	25.0	23.2	30.8	79.0	72.4	30	29				
3* (4-HPRO-D-Xylose	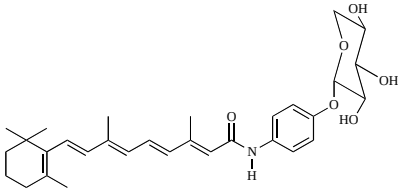		23.0*										
5* (4-HPROG)	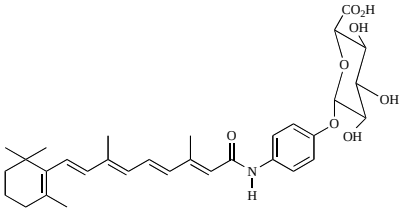		2.2*							66* 48**	66* 57**	0.83 0.71***	52*
6* (4-HPRC-D-Xylose)	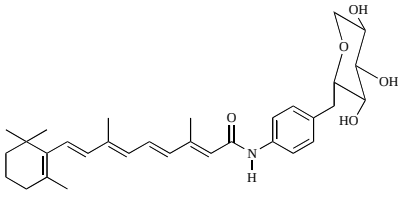		10.0*							42*	83*	1.25*	71*

(Table 4). Contd…..

7* (4-HPRC-D-Glucose)	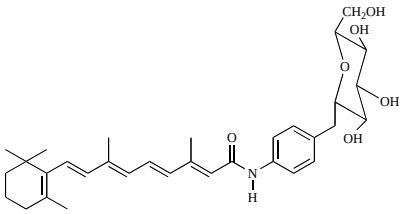		1.9*							71*	42*	0.75*	80*
8* (4-HPRCG)	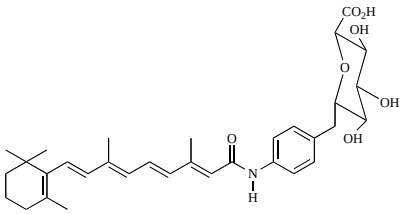		ND*[f] 6.5**							71* 55**	42* 27**	0.67* 0.36**	45*
Controls													
4-HPR	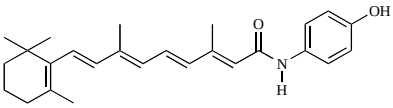	0.21	2.3 1.0* 0.3**	1.6	2.8	14.7	4.7	3.6	0.75	57*	83*	1.17*	27*
Control diet										41* 40**	92* 79**	1.50* 1.43**	
ATRA	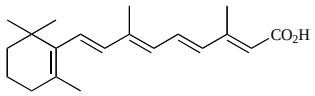												89*

Taken from Ref. [13-15].

[a]IC_{50} (μM), concentration inhibiting 50% proliferation of HL-60 myeloid leukemia (LeuC), MCF-7 breast cancer (BC), HT29 colon cancer (CC), and NCIH460 lung cancer (LC) cell lines, and normal MRC5 fetal lung fibroblasts (FLF) in stationary (stat) and exponential (expon) phases of growth, which represented cytotoxic and antiproliferative compound activities, respectively. Cell growth was measured using MTT assays after 7 days of treatment. Inhibition of 50% of the growth of donated human peripheral blood mononuclear (PBM) cells and that of the normal CEM T-lymphoblastoid cell line (CEM) were determined by propidium iodide staining and flow cytometry after 7-day treatments [13].

[b]Compounds at 1.0 mmol/kg diet were fed for 10 days to rats, which were then initiated with 7,12-dimethylbenz[*a*]anthracene (DMBA), after which compound-containing diet was continued for 10 more days. Rats were then switched to vehicle alone-containing diet for 85 days [14]. Latency, time to appearance of first tumor; incidence, % of rats with tumors at day 105; multiplicity, mean number of tumors per rat at day 105 [14]. This data is superscripted by one asterisk.

[c]Compounds at 2.0 mmol/kg diet were fed for 10 days to rats, which were then initiated with DMBA, after which compound diet was continued for 80 more days [15]. This data is superscripted by two asterisks.

[d]% label displaced was calculated from amount of label remaining bound to RARβ after 4 h using 10 μM compound or ATRA in competition with 2 nM [^{3}H]ATRA and was calculated from graphs in Fig. (**4**) of Ref. [14].

[e]Compound numbers refer to those in Ref. [13], unless marked with an asterisk, which refer to those in Ref. [14]. Data under the heading "BC" and marked by one or two asterisks refers to vehicle used in Ref. [14]. MCF-7 breast cancer cells were treated with compounds for an undefined time and then counted using a hemocytometer or Coulter counter after trypan blue staining for viability for comparison with the vehicle alone-treated control (DMSO* or EtOH**) to determine relative IC_{50} values.

[f]ND, not determined.

41 days. Both reduced the number of rats bearing tumors to 42% at the end of the study and the number of tumors/rat to 0.75 and 0.67, respectively, compared to the control values of 92% and 1.5 tumors/rat. The delays to first tumor appearance for 4-HPROG and 4-HPR were 66 and 57 days, respectively, and 66% and 83% of their treatment groups had tumors. 4-HPRC-D-xylose (**3***) was inactive as indicated by the 42-day latency in its treatment group. At 10 μM, all derivatives interacted with RARβ more effectively than 4-HPR did.

4-HPRCG was found to have the unique capability of inhibiting β-glucuronidase activity with an IC_{50} value of 236 μM to suggest that it may prevent the metabolic deactivation of ATRA *in vivo*, whereas 4-HPROG was found to function as a β-glucuronidase substrate (K_m = 184 μM) [15]. The actual target by which these compounds exert their anticancer effects remains to be identified although substantial evidence indicates that 4-HPR and its glycosyl derivatives/analogues inhibit cancer cell proliferation by a pathway(s) independent of interactions with the RAR subtypes. The peptidomimetic analogues of the 4-HPR glucuronide metabolite may have the potential for inhibiting cancer cell proliferation by an as yet undefined signaling pathway(s). Despite the robustness of the Curley–Clagett-Dame results [16], these compounds remain to be robustly investigated by other groups, who, perhaps, may have been negatively influenced by the unfavorable clinical trial results produced by 4-HPR in preventing the overall recurrence breast cancer [17].

Mechanistic Studies on 4-HPR

The ability of 4-HPR to induce apoptosis in a wide variety of cancer cell lines, including those for squamous cell carcinoma of the head and neck, neuroblastoma, leukemia, and breast, lung, and ovarian cancers, has been well documented [8-13]. The role of the RARs and RXRs in 4-HPR-mediated apoptosis remains somewhat controversial. Sheikh *et al*. [18] found that 4-HPR and its major metabolite *N*-(4-methoxyphenyl) retinamide (4-MPR) bound poorly to RARα, RARβ, and RARγ *in vitro* and only minimally acti-

vated the retinoid acid response element (RARE) and RXR response element in breast cancer cells. Metabolism of 4-HPR or 4-MPR to the conventional retinoids—ATRA and 9-cis-RA—was not detected in these cells [18]. In contrast, the Pfahl group in Fanjul *et al*. [19] report that 4-HPR activated transcription *via* RARβ and RARγ in CV-1 kidney cells and MCF-7 breast cancer cells. The extent of activation of the RARs by 4-HPR differed significantly depending on the RA response elements in the reporter assays. In support of these findings, Lovat *et al*. [20] reported that RARβ/γ antagonists, but not RARα antagonists, inhibited 4-HPR-mediated apoptosis in neuroblastoma cells. In contrast, unhydrolyzable 4-HPR analogues, which acted as potent apoptosis inducers, were shown to display weak binding to the RARs [16]. Although these compounds induced a number of ATRA-responsive genes through the RARs, they caused cell death through an RAR-independent mechanism [16]. Utilizing both wild-type and RARγ and RXRα-knockout embryonal carcinoma cell lines, Clifford *et al*. [21] reported that 4-HPR appeared to act through both RAR/RXR-dependent (differentiation-inducing) and RAR/RXR-independent (apoptosis-inducing) signaling pathways.

The induction of radical oxygen species (ROS) by 4-HPR has been documented to result in cell death and apoptosis [22, 23]. The central role of 4-HPR-mediated ROS generation as a crucial player in 4-HPR-induced cell death has been substantiated through the use of oxygen scavengers, which prevent 4-HPR-mediated ROS generation and apoptosis [24]. The 4-HPR-induced generation of ROS appears to occur through the loss of mitochondrial membrane potential [23]. Further investigations utilizing inhibitors of mitochondrial complexes I, II, and III suggested that 4-HPR-generated pro-oxidant activity was associated with redox metabolism occurring at the quinine-binding site in complex I and/or the center of complex III [23]. In respiratory-deficient clones, 4-HPR-mediated apoptosis was significantly inhibited, implying that mitochondrial respiration plays a major role in 4-HPR-mediated apoptosis [23].

Evidence has recently surfaced that the 4-HPR-mediated elevation of ROS resulted in the activation of the mitogen-activated protein/threonine kinase (MAPK) pathway in head-and-neck squamous cell carcinoma cell lines [25]. Exposure of these lines to 4-HPR led to a rapid rise in ROS levels followed by the rapid and prolonged phosphorylation and activation of JNK, p38, and ERK, whereas inhibition of 4-HPR-mediated ROS generation blocked MAPK activation. Moreover, inhibition of 4-HPR-mediated JNK phosphorylation and activation using the JNK-specific kinase inhibitor SP600125 blocked 4-HPR-induced apoptosis in these cells [25]. JNK inhibition also blocked cytochrome *c* release from the mitochondria, but had no effect on the 4-HPR-mediated increase in the permeability of the outer mitochondrial membrane and loss of membrane potential. Inhibition of p38 or ERK phosphorylation and activation or inhibition of protein kinase C activity upstream also blocked 4-HPR-induced apoptosis. These results suggest that the activation of protein kinase C by 4-HPR is responsible for the phosphorylation and activation of JNK, ERK, and p38 [25].

Exposure to 4-HPR has been found to result in the induction and expression of a number of genes that appear to play important roles in 4-HPR-mediated cell death. Exposure of SW 480 head-and-neck squamous cancer cells to 4-HPR resulted in the enhanced expression of death receptor (DR) 5 mRNA and protein [26]. DR5 on binding the tumor factor-related apoptosis-inducing ligand (TRAIL) becomes activated, leading to the subsequent activation of the extrinsic apoptosis pathway involving caspases-8 and 10. The combination of TRAIL and 4-HPR resulted in a significant increase in apoptosis induction over that noted with either agent alone [26]. The 4-HPR-induced increase in DR5 expression was found to be mediated through the CCAAT enhancer-binding protein homologous protein (CHOP, also called the GADD153 gene product) binding site located in the 5´-flanking region of the DR5 promoter. Silencing of CHOP expression or mutation of its DNA-binding site prevented the 4-HPR-induced increase in DR5 expression [26].

Several investigators demonstrated that exposure of cells to 4-HPR resulted in their upregulation of GADD153 expression [27, 28]. 4-HPR-treated nasopharyngeal carcinoma cells exhibited increased GADD153 expression as indicated by DNA microarray analysis, RT-PCR, and Western blot analysis. Enhanced GADD153 expression led to increased 4-HPR-mediated apoptosis [27, 28]. The dramatic increase in GADD153 promoter activity was not inhibited by the presence of the antioxidant vitamin C. Although GADD153 mRNA was found to be inherently unstable, the addition of 4-HPR and the associated increase in ROS levels significantly enhanced GADD153 mRNA stability. The increase in GADD153 stability was blocked by vitamin C and other antioxidants, as well as by the lipoxygenase inhibitor baicalein [25]. Further studies suggested that the 4-HPR-mediated increase in GADD153 mRNA levels involved the regions flanking its 5´-untranslated region (UTR) and 3´-UTR.

The endoplasmic reticulum (ER) of eukaryotic cells represents a separate metabolic compartment that plays vital roles as the site of membrane and secretory protein synthesis, the folding of proteins into native conformations, and protein posttranslational modifications, including the addition of oligosaccharides and disulfide bond formation [29]. 4-HPR induces ER stress and its associated responses by perturbing these important functions [30, 31]. These authors found that GADD153 mRNA was upregulated in malignant cells in response to 4-HPR-mediated ER stress [30, 31]. 4-HPR treatment resulted in the significant dilation of the ER as revealed by transmission electron microscopy [30]. XBP-1 is a transcription factor that becomes activated following splicing of its mRNA and translation. Both XBP-1 mRNA splicing and protein activation were induced by 4-HPR and promoted the unfolded protein response (UPR) and the upregulation of chaperone gene expression. These responses were inhibited by the antioxidant butylated hydroxyanisole [30]. Induction of the ER stress response was associated with the upregulation of genes encoding the chaperone proteins HSPAIA/heat shock protein (HSP) 70, HSP90/HSPAC, glucose-regulated protein 78 (GRP78/HSPAS/BiP), and GADD153 [30, 31]. Addition of 4-HPR to human squamous cell and ovarian carcinoma cell lines resulted in the induction of these ER stress-related genes and resulted in cell death

[30, 31]. Interestingly, the addition of an antioxidant prevented the induction of these genes [30]. Further examination revealed that, while HSP70 expression enhanced 4-HPR-mediated cell death, HSP90 inhibited it. The addition of the ER stress inhibitor salubrinal protected ovarian carcinoma cells from 4-HPR-induced apoptosis and inhibited the induction of the placental bone morphogenetic protein (PALP), whose expression has been found to enhance 4-HPR-mediated cell death [31].

Other mechanisms through which 4-HPR enhanced cell death in different cell types have been described [32-34] and include induction of ceramide production and cathepsin D release from lysosomes and inhibition of angiogenesis through 4-HPR-induced upregulation of bone morphogenetic protein-2 and macrophage inhibitory cytokine-1 levels [32-34]. These proteins accumulated in endothelial cells treated with 4-HPR and were found to specifically inhibit endothelial cell growth, migration, and invasion *in vitro* and to suppress angiogenesis in the Matrigel® plug assay *in vivo*.

The ability of 4-HPR to inhibit the growth of human ovarian and prostate carcinoma cells *in vivo* has been demonstrated in animal models [35, 36]. The potential clinical benefit of 4-HPR was demonstrated in several clinical trials. 4-HPR treatment of patients with resected erythroleukoplakia significantly prevented relapses and the occurrence of new lesions [37]. Administration of 4-HPR to premenopausal and postmenopausal women following primary treatment for breast cancer (surgery with or without radiation therapy) resulted in a significant risk reduction in the incidence of a second primary breast cancer in the premenopausal group [17].

ADAMANTYL-SUBSTITUTED RETINOID-RELATED COMPOUNDS (ARRS)

Overview

Members of this class have received various designations to distinguish them from the classical retinoids that function by interacting with the RAR and RXR subtypes. Among them are "AHPN", a nemonic for the prototype in this series, 6-[3′-(1-adamantyl)-4′-hydroxyphenyl]-2-naphthalenecarboxylic acid (CD437 in Fig. (**1**)), "AHPC" for (*E*)-4-[3′-(1-adamantyl)-4′-hydroxyphenyl]cinnamic acid (SR11298/ ST1926 in Fig. (**1**)), "RRM" for the retinoid-related molecules in the MX series originated by the Pfahl group, and "ARR" for the adamantyl-substituted retinoid-related molecules investigated by the Fontana and Dawson groups.

Research in this area began in the early 1990s after an observation by a Dawson group member, Ms. Wan-ru Chao (SRI, Menlo Park, CA), that treatment of trans-retinoic acid (ATRA)-sensitive MCF-7 breast cancer cells with RARγ-selective AHPN (first labeled CD437 [38]) caused the cells to detach from the culture plate, whereas the other RARγ-selective transcriptional agonists did not produce the same robust effect. AHPN is the parent phenol of the drug adapalene (Differin™), which was developed by CIRD-Galderma (Sofia Antipolis, France) for topical treatment of mild-to-moderate acne. Further studies after the initial report of the RARγ selectivity of AHPN [38] had not been pursued by Galderma. On the basis of its MCF-7 cell death-inducing behavior, Dr. Joseph A. Fontana (Veterans Administration Medical Center and Wayne State University School of Medicine, Detroit, MI) evaluated AHPN in ATRA-resistant MDA-MB-231 breast cancer cells, and then Dr. Marcia I. Dawson (Sanford–Burnham Medical Research Institute, La Jolla, CA) investigated its effects on the ATRA-resistant OVCAR-3 ovarian cancer cell line [39]. The Fontana group found that AHPN induced apoptosis as evidenced by caspases-9 and 3 activation, PARP cleavage, and acridine orange staining [40]. Dr. Fontana next initiated a collaboration with Galderma to obtain AHPN/CD437 for further evaluation. These studies led him to be listed as the inventor on a Galderma patent claiming the use of CD437 for the treatment of cancer [41]. Chao *et al*. [39] determined that anchorage-independent growth inhibition of OVCAR-3 cells by a series of retinoids did not correlate with their transactivation of either RARα or RARγ and that of the retinoids evaluated AHPN was the most potent (IC_{50} = 0.13 μM after 9 days of treatment) followed by its 5-hydroxyphenyl analogue SR11364 (IC_{50} = 0.71 μM). The Fontana group also demonstrated that AHPN induced the expression of various genes and cell-cycle arrest before inducing apoptosis and that these activities were independent of its interactions with the RARs [40, 42-50]. The cell-cycle arrest and apoptotic effects of AHPN were also confirmed by other groups using a variety of cancer cell lines [51-64].

The pathway by which the adamantyl-substituted retinoid-related molecules evolved from ATRA is illustrated in Fig. (**2**).

The original report by Fontana and Dawson [40] in 1995 may have stimulated Dr. Magnus Pfahl (then at the Sidney Kimmel Cancer Center and Maxia Pharmaceuticals, San Diego, CA) to enter this field [65-70]. Dr. Pfahl, who had formerly collaborated with the Dawson group, continued to collaborate with Galderma, and then founded Maxia Pharmaceuticals with Galderma and evaluated both CIRD and Maxia AHPN analogues for their anticancer activities. One analogue did enter clinical trials for topical treatment of cervical cancer before Maxia was acquired by Incyte Genomics (Palo Alto, CA) in 2003. Incyte underwent restructuring in 2004 and closed the San Diego facility. The current status of the Maxia patents has not been reported. Dr. F. Javier Piedrafita (Torrey Pines Medical Research Institute, San Diego, CA), who began investigating AHPN and its analogues as a postdoctoral fellow in the Pfahl laboratory, has continued independent research in the area, most recently in collaboration with the organic chemistry group of Dr. Angel de Lera (Universidade de Vigo, Vigo, Spain).

Sigma-Tau Pharmaceuticals (Rome, Italy) also entered the field and developed AHPC (termed ST1926) for treatment of leukemia and ovarian cancer [71-73]. Several of the company's biological and mechanistic studies on ST1926 were performed in collaboration with Dr. Enrico Garattini of the Instituto di Ricerche Farmacologiche Mario Negri (Milan, Italy) [74-77]. Although active in inducing apoptosis of ovarian cancer cells in culture, the efficacy of ST1926 at tolerable doses was deemed to be low-to-moderate in murine models [78]. However, its combination with cisplatin produced a greater than additive effect at reducing ovarian tumor volume with only ≤ 10% loss in body weight in the

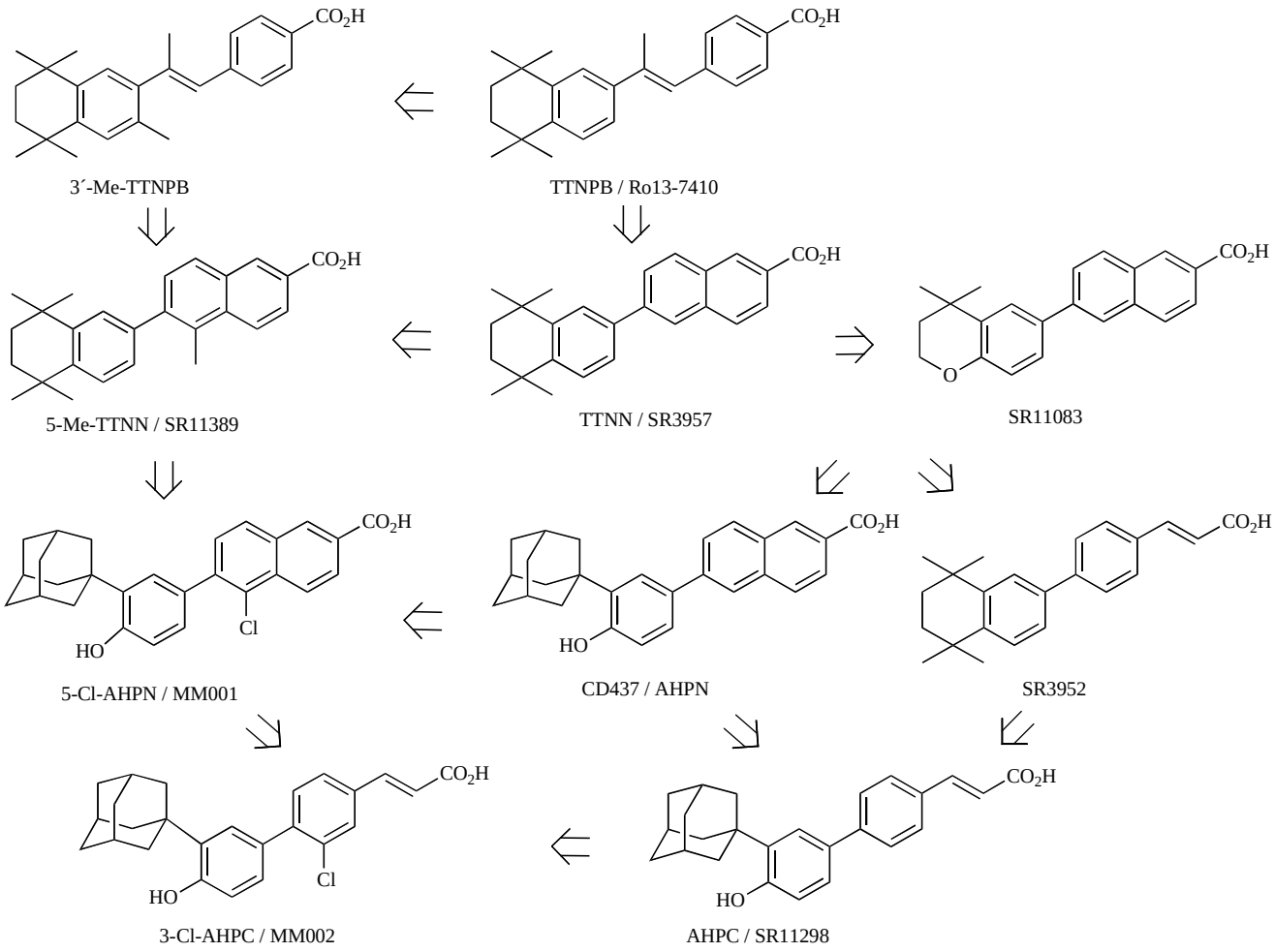

Fig. (2). Evolution of the AHPN analogues 6-[3′-(1-adamantyl)-4′-hydroxyphenyl]-5-chloro-2-naphthalenecarboxylic acid (5-Cl-AHPN / MM001), (*E*)-4-[3′-(1-adamantyl)-4′-hydroxyphenyl]cinnamic acid (AHPC / SR11298), and its 3-chloro analogue (3-Cl-AHPC / MM002) from (*E*)-4-[5,6,7,8-tetrahydro-5,5,8,8-tetramethyl-2-naphthyl)propenyl]benzoic acid (TTNPB / Ro13-7410) and 3′-Me-TTNPB by the Dawson group.

mouse. Similar synergistic results for ST1926 were obtained in combination with the histone deacetylase inhibitor *N*-hydroxy 3-(4´-hydroxybiphenyl-4-yl)acrylamide [79]. The phase I clinical trial results of variable and low plasma levels of ST1926 and its glucuronidation [80] suggest that structural modifications of ST1962 may be useful. Future clinical trials to be sponsored by Sigma-Tau have been designed to use ST1926 in combination with cisplatin for treatment of ovarian cancer. Combination treatment was expected to permit the use of ST1926 at lower and pharmacologically achievable doses [78].

The collaborating Dawson and Fontana groups undertook mechanistic and synthetic studies with NCI grant support to identify an AHPN analogue suitable for clinical translation to cancer treatment [48, 81-83]. The Dawson group had originally synthesized AHPC (labeled SR11298) in 1992 in an effort to reduce the toxicity of AHPN, which appeared to be associated with its retinoid activity. Evaluation using the retinoid-sensitive TREpal response element in a reporter assay indicated that AHPN behaved as an RARβ/γ-selective transcriptional agonist at 1 μM. AHPC was designed to incorporate elements that previously were found to reduce retinoid activity in analogues of 6-(5,6,7,8-tetrahydro-5,5,8,8-tetramethylnaphth-2-yl)-2-naphthalenecarboxylic acid (TTNN), namely replacement of its tetrahydrotetramethylnaphthalene ring (TTN) by a 3-(1-adamantyl)-4-hydroxyphenyl group and its 6-substituted naphthalene-2-carboxylic acid moiety by a 4-substituted *E*-cinnamic acid. Unfortunately, administration of AHPC at levels that were effective against breast cancer xenograft growth in murine models also produced toxic side effects in mice such as > 10% weight loss that were outside the NCI guidelines for cancer monotherapy. Thus, the search for less-toxic analogues was continued [84].

5-Cl-AHPN and 3-Cl-AHPC were identified next [85-87]. 3-Cl-AHPC was the less toxic of the two analogues in mice, and both were less toxic than AHPC. The insertion of the chloro group ortho to the diaryl bond in 5-Cl-AHPN considerably reduced its retinoid activity profile by eliminating transcriptional activation activity (agonism) for all three

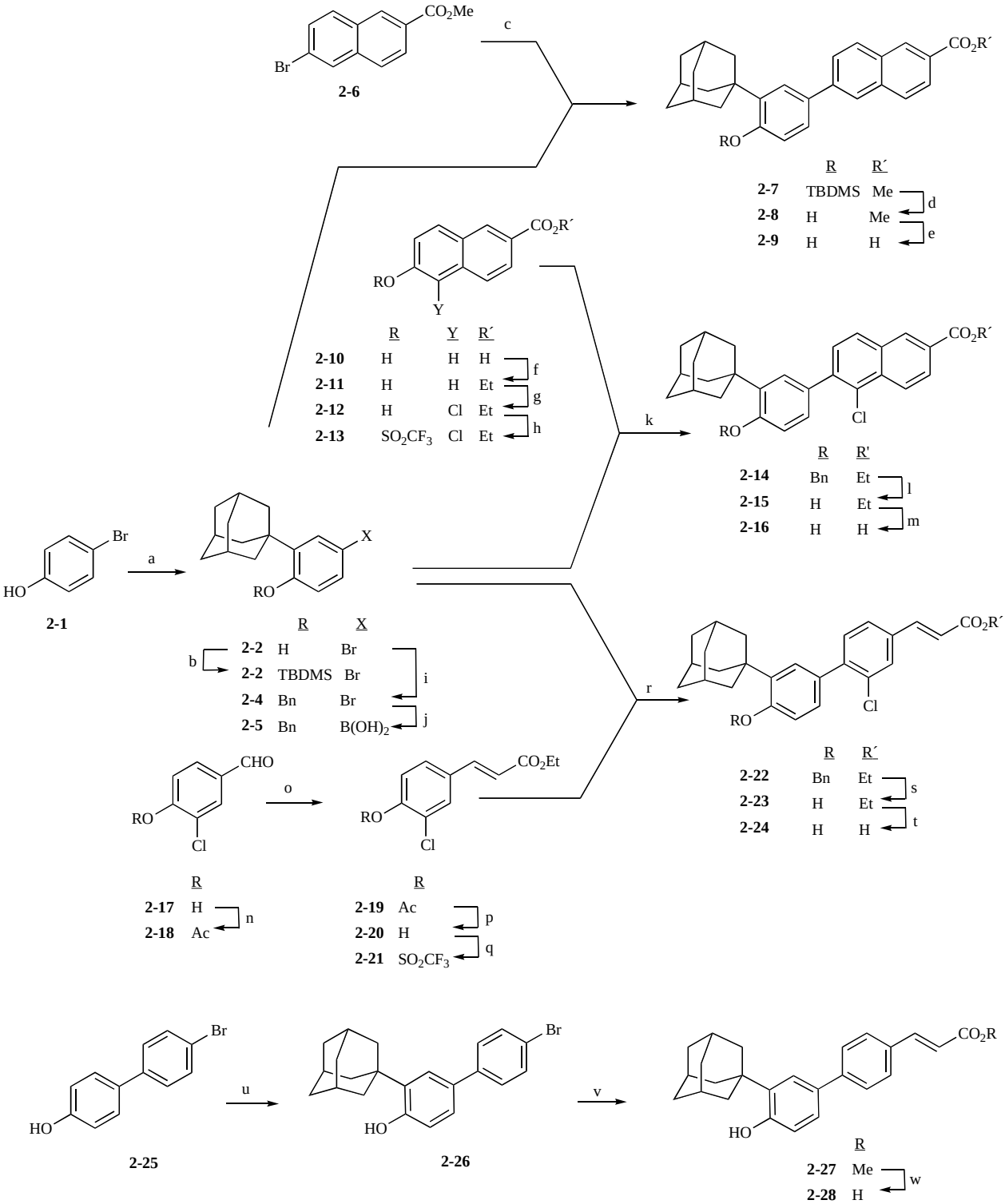

Scheme 2. (a) 1-Adamantanol, H_2SO_4, CH_2Cl_2 (80–86%) [84, 92]. (b) *t*-$BuMe_2SiCl$, 4-Me_2N-pyridine, Et_3N (86%) [92]. (c) **2-6**, Mg, THF, rt to 40 °C; $ZnCl_2$; THF; **2-3**, $NiCl_2$, $(Ph_2PCH_2)_2$, (90%) [92]. (d) $(n\text{-}Bu)_4NF$, THF (99%) [92]. (e) aq NaOH, MeOH, reflux; 6 N HCl (79%) [92]. (f) EtOH, H_2SO_4, reflux (85%) [98]. (g) SO_2Cl_2, HOAc, 70°C (62%) [98]. (h) $(CF_3SO_2)_2O$, pyridine, CH_2Cl_2, 0 °C to 20 °C (78%) [98]. (i) $PhCH_2Br$, K_2CO_3, THF (78%) [84]. (j) *n*-BuLi, THF; $(i\text{-}PrO)_3B$, THF; dil HCl (81%) [84]. (k) **2-13**, **2-5**, $Pd(Ph_3P)_4$, LiCl, 2 M Na_2CO_3, DME (56%) [98]. (l) BBr_3, CH_2Cl_2, –78 °C; H_2O (71%) [98]. (m) aq NaOH, EtOH, reflux; H_3O^+ (95%) [98]. (n) Ac_2O, pyridine, CH_2Cl_2, 0 °C to 20 °C (92%) [88]. (o) $(EtO)_2P(O)CH_2CO_2Et$, K_2CO_3, THF (87%). (p) MeOH, K_2CO_3; dil HCl (87%). (q) $(CF_3SO_2)_2O$, pyridine, CH_2Cl_2, 0 °C to 20 °C; dil HCl (98%). (r) **2-21**, **2-5**, $Pd(Ph_3P)_4$, 2 M Na_2CO_3, DME, reflux (79%). (s) BBr_3, CH_2Cl_2, −78 °C; H_2O (92%). (t) dil NaOH, EtOH, 85 °C; H_3O^+ (85%). (u) 1-Adamantanol, H_2SO_4, HOAc (100%) [71]. (v) $H_2C{=}CHCO_2Me$, $(2\text{-}MePh)_3P$, $Pd(OAc)_2$, Et_3N, 100 °C (98%) [71]. (w) $LiOH{\cdot}H_2O$, THF, H_2O, 25 °C; 2 N HCl (94%) [71].

RAR subtypes and binding to RAR subtypes α and β, and reducing binding to RARγ. However, 3-Cl-AHPC was not evaluated in the retinoid transactivation assay to avoid conflicts with the Ligand Pharmaceuticals' license to the Sanford–Burnham Institute to only use this retinoid receptor transactivation assay for academic research purposes. Its use on 3-Cl-AHPC would have blocked the possibility for clinical translation. To permit such translation, the Institute submitted a patent application claiming 3-Cl-AHPC and its analogues [88]. The Dawson and Fontana groups have since identified promising active and nontoxic analogues that demonstrated robust anticancer activity in animal models. The methyl ether of AHPC was patented by Sigma-Tau for use in treating acne [89].

Synthesis

The syntheses of 5-Cl-AHPN and 3-Cl-AHPC by the Dawson group [90, 91] are illustrated in Scheme **2** as examples of how ARRs have been prepared. Notable steps in these syntheses are the Friedel-Crafts monoadamantylation of 4-bromophenol, the Suzuki coupling of 3-(1-adamantyl)-4-benzyloxyphenylboronic acid with aryl bromides or triflates to form the phenyl–cinnamyl bond, the selective 5-chlorination of 6-hydroxy-2-naphthanoate with sulfuryl chloride, and the Heck coupling to introduce the cinnamic acid trans-double bond. The Galderma [92], Sigma-Tau [71], and de Lera groups [93, 94] have reported syntheses of analogues, several of which are also included in Scheme **2**.

Structure–Activity Relationships

Despite the wealth of analogues of AHPN and AHPC generated thus far by the Galderma [92], Dawson–Fontana [90, 91], Maxia [66], and Sigma-Tau groups [71], and more recently by the de Lera–Piedrafita groups [93, 94], the critical pharmacologic determinants for anticancer activity continue to be the 3′-(1-adamantyl), the 4′-phenolic hydroxyl, and the carboxylic acid groups. These groups are logical if the nuclear receptor small heterodimer partner (SHP) is the actual target for the apoptotic activity of AHPN and AHPC [81, 82, 90]. AHPN binds to SHP protein with a K_D of 2.9 ± 0.6 nM to suggest a highly compatible fit [82]. Docking to a model of SHP [95] constructed by the group of Dr. Roberto Pellicciari (Universita′ degli Studi di Perugia, Perugia, Italy) from the homologous ligand-binding domain of ultraspicle, the insect version of the human retinoid X receptor, supports the compatibility between 3-Cl-AHPC and the SHP receptor pocket [91]. AHPN, AHPC, and their analogues were the first synthetic ligands discovered for SHP. A natural ligand for SHP remains to be identified.

The structure-activity data on the AHPN and AHPC analogues in Tables **5** through **10** are presented in terms of the order of their synthesis. Initial studies by Galderma focused on the retinoid activity of AHPN and its analogues (Table **5**). Unfortunately, patents claiming retinoid nuclear receptor transactivation assays using reporter constructs in transfected cells had been issued to the Salk Institute and then licensed to Ligand Pharmaceuticals (San Diego, CA) [96, 97]. Therefore, probably because of potential litigation issues, only RAR subtype binding data on these adamantyl-substituted retinoids was reported by Galderma [92] for use in making correlations with their activities in the retinoid-sensitive F9 murine teratocarcinoma cell differentiation assay. Analysis of this data only suggests that interactions of these compounds with RARγ could have a role in F9 cell differentiation but is more rigorous in establishing that interactions with RARα and RARβ do not. Interestingly, both 4-HPR (**1** in Table **1**) and 4-MPR (**50** in Table **1**) were more active than ATRA in this F9 cell assay [92]. The AHPN analogue having a 4′-(3-hydroxypropyl) group (**9** in Table **5**, EC_{50} 7.5 nM) and the TTNPB analogue **20** (EC_{50} 1 nM) having an *E*-ethenyl bridge were the most potent in the F9 assay to suggest that they functioned as retinoids.

SAR investigations on the AHPN and AHPC analogues identified by the Dawson and Fontana groups [91, 98] focused on apoptotic activity in leukemia and breast cancer cell lines (Table **6**). ATRA-resistant HL-60R human myeloid leukemia cells were far more sensitive to these compounds than ATRA-resistant MDA-MB-231 breast cancer cells with the latter requiring 72 h rather than 24 h to induce apoptosis of about 50%. The most active apoptosis inducers were AHPN (**13** in Table **6**), its 5-chloro (**14**), 5-methyl (**17**), and 3-chloro (**9***) analogues, and AHPC (**15**) followed by 3-Cl-AHPC (**1**), 3-methyl-AHPC (**43**), and 2-adamantyl-AHPC (**40**). Other variations at the 3′-phenyl ring position led to appreciable or total loss of apoptotic activity. The active compounds were also able to inhibit the growth and induce the apoptosis of human microvascular endothelial (HMVE) cells, thereby suggesting antiangiogenic activity. Shifting the position of the 4′-OH group to the 5′ and 6′-positions on the phenyl ring (**32** and **34**, respectively) eliminated apoptotic activity, whereas its replacement by 4′-methoxy in AHPN analogue **19** and 4′-amino in 3-Cl-AHPC analogue **3** reduced activity. Substitutional variations at the 5-naphthalene ring position of AHPN and the 3-cinnamyl phenyl ring position of AHPC indicated that hydrogen produced the most active compounds (**13** and **1**, respectively), followed by chloro or bromo and then methyl. The 3-ethoxy group (**13***) further reduced activity, whereas 3-acetamidopropyloxy-AHPC (3-A-AHPC, **10***) was devoid of apoptotic activity but still induced cell-cycle arrest to suggest two signaling pathways were being modulated by these compounds [98].

Much of the early reported research on the Maxia series compounds was related to their inhibition of cancer cell growth in association with RARγ interaction [66-70]. Of the three Maxia compounds shown in Table **7**, at 2 μM 2-[3′-(1-adamantyl)-4′-methoxyphenyl]benzimidazole-6-carboxylic acid (MX-2870-1) was the most highly active (≥ 95% growth inhibition) in four ATRA-resistant cancer cell lines and inhibited ATRA-resistant Du145 prostate cancer cell growth by 88%, whereas the AHPN analogue MX-3350-1 having a 3′-(1-adamantyl)-4′,5′-dioxamethylenephenyl ring was the most active against the ATRA-resistant BT-20 breast and Calu-6 lung cancer cell lines (69% and 63% growth inhibition, respectively) but ineffective against the ATRA-resistant WiDr colon cancer and Du145 prostate cancer cell lines and only modestly active (44% inhibition) against the SKOV-1 ovarian cancer line [66].

SAR studies by Sigma-Tau were focused on modifications at the 4′ and 5′-phenyl ring positions and on the double bond of the cinnamyl group of AHPC and evaluations in

Table 5. Adapalene Analogues Bind Retinoic Acid Receptor Subtypes and Inhibit F9 Teratocarcinoma Cell Differentiation

AHPN series	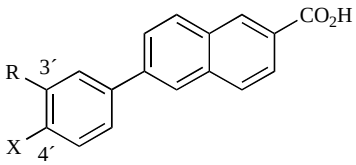			Binding K_i (nM)[a]			F9 cell differentiation[b]
Cmpd No[c]	**R**	**X**		**RARα**	**RARβ**	**RARγ**	**EC_{50} (nM)**
5	1-Ad[e]	OMe		1,100	34	130	37
6	1-Ad	$O(CH_2)_5CH_3$		>10,000	>10,000	>10,000	NA[f]
7	1-Ad	OH		6,500	2,480	77	33
8	1-Ad	CH_2OH		>10,000	156	386	460
9	1-Ad	$(CH_2)_3OH$		695	21	72	7.5
10	1-Ad	$CH(OH)CH_2OH$		>10,000	288	153	73
11	1-Ad	$CH_2CH(OH)CH_2OH$		>10,000	158	34	100
12	1-Ad	$OCH_2CH(OH)CH_2OH$		5,000	89	151	83
13	1-Ad	CO_2H		>10,000	>10,000	>10,000	2,000
1	*t*-Bu	OMe		6,500	36	426	200
2	*t*-Bu	OH		>10,000	3,550	200	NA
3	1-Me-cyclohexyl	OMe		1,120	26	160	150
4	1-Me-cyclohexyl	OH		>10,000	660	121	175
TTNPB series	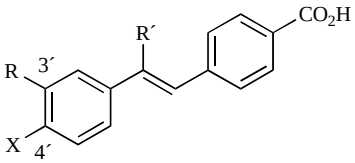						
Cmpd No[c]	**R**	**X**	**R´**				
18	1-Ad	OMe	Me	460	105	95	100
19	1-Ad	OH	Me	1,144	1,245	53	66
14	*t*-Bu	OMe	Me	130	12	13	30
15	*t*-Bu	OH	Me	834	105	85	NA
16	1-Me-cyclohexyl	OMe	Me	420	17	29	30
17	1-Me-cyclohexyl	OH	Me	1,056	90	27	300
20	1-Ad	OH	H	610	70	20	1
Controls							
ATRA	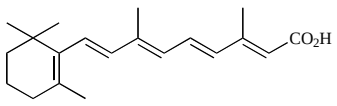			16	7	3	200
TTNN[d]	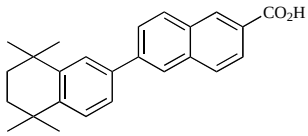			580	13	40	15

(Table 5). Contd…..

TTNPB[d]	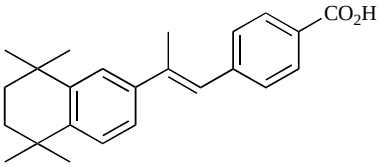	21	5	5	0.78
TTAB[d]	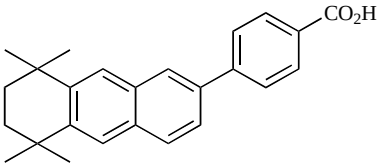	5.3	3	2	0.46

Taken from Ref. [92].

[a]K_i values for binding to the retinoic acid receptor (RAR) subtypes were determined in competition with 2 nM [^{3}H]TTAB.

[b]EC_{50}, concentration required to induce 50% differentiation of murine F9 teratocarcinoma cells, which was measured by secreted levels of induced plasminogen activator after 3 days treatment of cells grown in presence of 15% serum.

[c]Compound numbers taken from Ref. [92].

[d]TTNN, 6-(5,6,7,8-tetrahydro-5,5,8,8-tetramethyl-2-naphthyl)-2-naphthalenecarboxylic acid; TTNPB, (*E*)-4-[2-(5,6,7,8-tetrahydro-5,5,8,8-tetramethyl-2-naphthyl)propenyl]benzoic acid; TTAB, 4-(5,6,7,8-tetrahydro-5,5,8,8-tetramethyl-2-anthracenyl)benzoic acid.

[e]Ad, adamantyl group.

[f]NA, not active.

Table 6. Analogues of AHPN and Their Effects on Human Microvascular Endothelial (HMVE) Cell Growth and Induction of Leukemia and Breast Cancer Cell Apoptosis, and Analogues of AHPC and Their Effects on Cancer Cell Growth, Leukemia Cell Growth and Apoptosis, and Binding Affinities to the Orphan Nuclear Receptor Small Heterodimer Partner

AHPN series	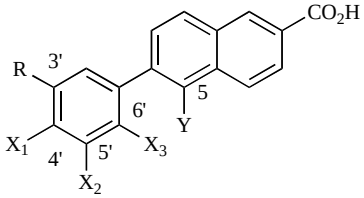					**HMVE growth inhibition at 7 days[a]**		**Apoptosis (%)[b]**			
								LeuC at 24 h		**BC at 96 h**	
Cmpd No[c]	**R[d]**	**X_1**	**X_2**	**X_3**	**Y**	**% at 0.5 μM**	**IC_{50} (μM)**	**0.1 μM**	**1.0 μM**	**1.0 μM**	**2.0 μM**
13 (AHPN)	1-Ad	OH	H	H	H	70	0.33	73	98	26	46
17 (5-Me-AHPN)	1-Ad	OH	H	H	Me	65	0.34	29	70	28	43
14 (5-Cl-AHPN)	1-Ad	OH	H	H	Cl	45	>0.5	62	94	21	41
18	1-Ad	H	H	H	H	36	>0.5	2	2	2	7
19	1-Ad	OMe	H	H	H			3	95		
20	1-Ad	OMEM	H	H	H			ND[e]	21		
21	*t*-Bu	OH	H	H	H	10	>0.5				
22	OMe	OH	H	H	Me			–4	7	5	7
23	2-Ad	OH	H	H	H	35	>0.5	0	0		
24	2,4,6-Me_3-Ph	OH	H	H	Me	17	>0.5	0	0		
25	3,3,5,5-Me_4-cyclohexyl	OH	H	H	H	50	0.5	26	60	10	49
26	$Me_2C{=}CH(CH_2)_2CMe{=}CHCH_2$	OH	H	H	H			ND	0		
27	1-(1-Ad)Et	OH	H	H	H	30	>0.5	ND	0		

(Table 6). Contd…..

28	TTN	OH	H	H	Me	60	0.6	0	0		
29	4aβ,8aα-decalin-2α-yl	OH	H	H	H	0	>0.5	ND	0		
30	4a,8aα-decalin-2β-yl	OH	H	H	H			ND	0		
31	4aα,8a-decalin-1α-yl	OH	H	H	H	10	>0.5	ND	0		
32	1-Ad	H	OH	H	H				ND	0	
33	1-Ad	H	OMe	H	H				ND	20	
34	1-Ad	H	H	OH	H				ND	0	
35	1-Ad	H	H	OMe	H				0	ND	
36	1-Ad	OH	OH	H	H				ND	0	
37	1-Ad	OH	OMe	H	H				ND	0	
38	OMe	1-Ad	H	H	H				0	ND	
39	$Me_2C(CH_2)_2CMe_2$		H	CH_2OH	H				ND	0	
9* (3-Cl-AHPN)	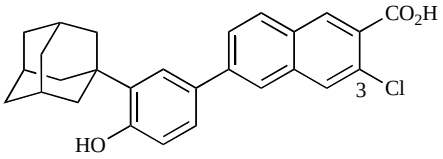								90		
Control											
16 (ATRA)	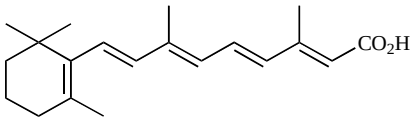					10	>0.5	0	0	0	0
3X-AHPC series	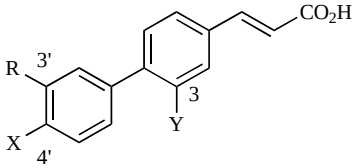										
Cmpd No[c]	**R**[d]	**X**	**Y**								
15 (AHPC)	1-Ad	OH	H			90	0.1	90	98	53	58
1 (3-Cl-AHPC)	1-Ad	OH	Cl					51	94	31	43
40	2-Ad	OH	H					2	90	20	47
41	2,3,3-Me_3-norbornyl	OH	H			40	>0.5	2	2		
42	3α-pentylbicyclo[2.2.2]octyl	OH	H					0	0		
43	TTN	OH	H					ND	0		
12* (3-Me-AHPC)	1-Ad	OH	Me					10	95	5	30
13* (3-EtO-AHPC)	1-Ad	OH	OEt					0	29		
10* (3-A-AHPC)	1-Ad	OH	$O(CH_2)_3NHAc$					0	0	0	1

(Table 6). Contd…..

3-Cl-AHPC series	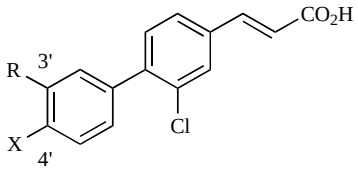		**50% growth inhibition (IC_{50}, μM)[f]**				**AML apoptosis at 48 h (%)[b]**		**SHP binding (%)[g]**
Cmpd No[c]	**R[d]**	**X**	**BC**	**LC**	**PC**	**AML**	**1 μM**	**5 μM**	**50 μM**
1 (3-Cl-AHPC)	1-Ad	OH	0.95	0.4	0.48	1.4	30	55	100
2	1-Ad	NHAc	>5	>5	5	>5	3	7	43
3	1-Ad	NH_2	4.0	6.0	1.3	5.0	10	40	61
4	1-Ad	F	67	6.0	16	>5	0	0	90
5	H	F	>100	47	>100	>5	0	0	39
6	*t*-BuCC	OH	>10	>10	>10	>5	0	0	59
7	2,6-Me_2-Ph	OH	>10	>10	>10	>5	0	0	29
8	1-Noradamantyl	OH	9.8	6.8	7.9	0.92	2	16	85
9	1-Me-cyclohexyl	OH	>5	3.9	8.0	>5	0	0	77
10	5,5-Me_2-1-Ad	OH	>5	3.6	>5	>5	0	0	103
11	2-Me-1,3-dithian-2-yl	OH	>20	>20	>20	>5	5	5	40
12	1,1-Et_2-propyl	OH	>5	>5	>5	>5	3	4	90
Control									
13 (AHPN)	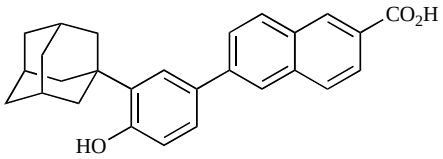								100

Taken from Ref. [91, 98].

[a]Human microvascular endothelial (HMVE) cells were treated for 7 days with 0.5 μM compound or vehicle alone in medium containing 5% heat-inactivated fetal bovine serum (FBS) before cell growth was determined using relative fluoresence after Alamar blue staining.

[b]Apoptosis of retinoid-resistant HL-60R myeloid leukemia cells (LeuC), MDA-MD-231 breast cancer (BC), and KG-1 acute myeloid leukemia (AML) cells was determined by acridine orange staining after treating cells for 24 h, 96 h, and 48 h, respectively, with the indicated concentrations of compound in medium containing 5% FBS.

[c]Compound numbers correspond to those reported in Ref. [91] except those followed by an asterisk, which correspond to those in Ref. [98].

[d]Ad, adamantyl; TTN, 5,6,7,8-tetrahydro-5,5,8,8-tetramethyl-2-naphthyl.

[e]ND, not determined.

[f]IC_{50} values for growth inhibition of MDA-MB-231 breast cancer (BC), H292 lung cancer (LC), DU145 prostate cancer (PC), and KG-1 acute myeloid leukemia (AML) cells were calculated from dose-response curves after treating for 72 h (BC, LC, and PC) or 48 h (AML). Relative cell numbers were determined by counting using a hemocytometer or by conducting MTT assays.

[g]Small heterodimer partner (SHP) binding (%) represents radiolabel displaced from SHP in the presence of 5 nM [5,5′-$^3H_2$]AHPN plus 50 μM compound with displacement by 50 μM 3-Cl-AHPC regarded as 100%.

IGROV-1 ovarian cancer and NB4 acute myeloid leukemia cell lines [99]. The IC_{50} values for growth inhibition by these analogues were similar in both lines (Table **8**). Interestingly, the levels of apoptosis (%) induced in IGROV-1 cells by these analogues at concentrations corresponding to their 80% growth inhibition (IC_{80}) values did not correlate with the IC_{50} values found for their growth inhibition to suggest that more than one pathway was involved. An early event (at 6 h) was found to be the phosphorylation of histone γ-H2AX, replication protein A, and p53. The phosphorylation of these proteins has been associated with the cellular response to DNA damage. AHPC (**1** in Table **8**), its methyl ether (**9**), 5′-aminomethyl-AHPC (**15**), 5′-hydroxymethyl-AHPC (**21**), and the 4′,5′-dioxamethylene analogue (**31a**) induced similar levels of apoptosis (45–55%), whereas the 5′-hydroxy analogues of the methyl ether of AHPC (**24**) and the 4′,5′-dioxaethylene analogue (**31b**) were less active with 20% and 30% apoptosis induced, respectively. Introduction of an α-bromo group on the cinnamyl double bond in **10c** and **35** or its replacement by acetylene in **11** and **34** reduced cancer cell growth inhibition compared to that of the methyl ether of AHPC (**9**).

The de Lera and Peidrafita groups produced a series of analogues of Maxia's MX-781 (Table **9**) that merged the chalcone ring system, which was first introduced by Professor Koichi Shudo and colleagues (University of Tokyo,

Table 7. AHPN Analogues Derived from Adapalene, Their Effects on Cancer Cell Growth, and Activation of RARγ in Reporter Construct Assays Containing Different Retinoic Acid Response Elements

AHPN[a] series		Cell growth at 2 μM cmpd after 5 days (% vehicle control)[b]					RARγ activation on RARE in gene promoter at 2 μM cmpd (%)[c]		
Cmpd	**Structure**	**BC**	**CC**	**LC**	**OC**	**PC**	**CRBP-I**	**ApoA1**	**DR5**
MX-90-1	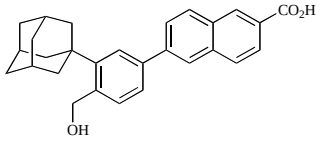	9	104	91	104	46	56	81	29
MX-2870-1	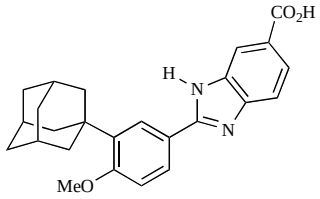	4	1	5	4	12	74	244	85
MX-3350-1	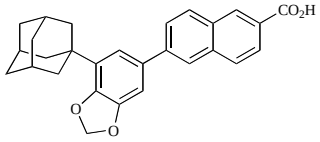	31	99	37	56	100	81	145	56
Controls									
ATRA[d]	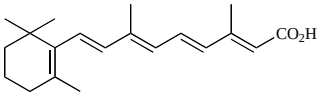	97	124	82	103	115	100	100	100
Cisplatin		6	8	7	0	0			

Taken from Ref. [66].

[a]AHPN, 6-[3-(1-adamantyl)-4-hydroxyphenyl]-2-naphthalenecarboxylic acid.

[b]Cell growth relative to control for BT-20 breast cancer (BC), WiDr colon cancer (CC), Calu-6 lung cancer (LC), SKOV-3 ovarian cancer (OC), and Du145 prostate cancer (PC) cells treated with 2 μM compound compared to that of 2 μM ATRA and 40 μM cisplatin as determined using a colorimetric assay. Cell growth conditions in assays and treatment times were not described.

[c]Transcriptional activation of RARγ on three different RARE–chloramphenicol acetyl transferase (CAT) reporter constructs by 2.0 μM compound compared to that of 2.0 μM ATRA as 100% in an unspecified cell line.

[d]ATRA, all-trans-retinoic acid.

Table 8. AHPC Analogues and Their Effects on Leukemia and Ovarian Cancer Cell Growth, and Ovarian Cancer Cell Apoptosis and DNA Damage Response

AHPC series	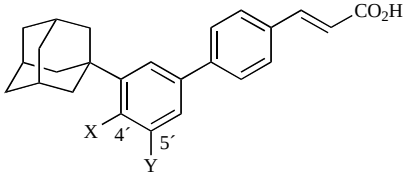		50% inhibition of cell growth (IC_{50}, μM)[a]		OC cell response to cmpd at IC_{80}			
					Apoptosis at 72 h[b]	DNA damage-induced phosphorylation at 6 h[c]		
Cmpd No[d]	**X**	**Y**	**LeuC**	**OC**	**(%)**	**γ-H2AX**	**RPA**	**p53**
1 (AHPC)	OH	H	0.08	0.23	51	+2	+1	+2
5	H	H	ND[e]	18.8				
6	H	OH	1.2	1.31				
9	OMe	H	1.1	1.19	47	+4	+1	+3
13	OH	CH_2NHAc	0.99	1.24				

(Table 8). Contd…..

15	OH		CH_2NH_2			0.18	0.45	55	+2	+3	+1
20	OMe		OMe			1.89	0.71				
21	OH		CH_2OH			0.19	0.76	45	+2	+3	+2
22	OH		CHO			1.61	1.64				
24	OMe		OH			0.55	0.57	20	+1	+1	+1
27	OH		OMe			0.27	0.52				
31a	OCH_2O					0.26	0.39	50	+3	+1	+2
31b	$O(CH_2)_2O$					0.11	0.23	30	+2	+2	+3
Cinnamic double bond series	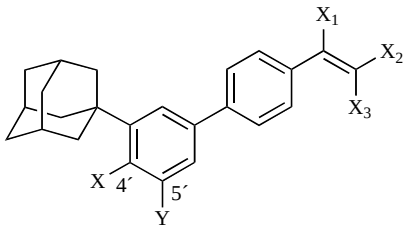										
Cmpd No[d]	**X**	**Y**	**X_1**	**X_2**	**X_3**						
10d	OMe	H	H	CO_2H	Br	41	30.6				
10c	OMe	H	H	Br	CO_2H	17.9	>>20				
11	OMe	H	--	--	CO_2H	ND[e]	1.7				
34	OCH_2O		--	--	CO_2H	2.0	3.6				
35	OCH_2O		H	Br	CO_2H	72.3	36.6				

Taken from Ref. [99].

[a]NB4 acute myeloid leukemia cells (LeuC) were treated for 24 h, and growth inhibition was assessed at 72 h. IGROV-1 ovarian cancer cells (OC) were treated for 72 h before growth inhibition was assessed. The assay used was not described.

[b]Only **1**, **9**, **15**, **21**, **24**, **31a**, and **31b** were assayed for IGROV-1 ovarian cancer cell (OC) apoptosis, which was determined by morphological change using the TUNEL assay after propidium iodide staining.

[c]Relative phosphorylation (0 to +4) was estimated from western blot data given in Fig. (**2**) of Ref. [99]. Phosphorylation levels overall were highest for γ-histone (H) 2AX, followed by p53(Ser15), and then replication protein A (RPA), using β-tubulin as the loading control. Cell growth conditions and serum levels were not described.

[d]Compound numbers refer to those in Ref. [99].

[e]ND, not determined.

Tokyo, Japan) in synthetic retinoids such as (*E*)-4-{3′-[3,5-di(*t*-butyl)phenyl]-3′-oxopropenyl}benzoic acid (Ch55) and (*E*)-4′-[3-oxo-(5,6,7,8-tetrahydro-5,5,8,8-tetramethyl-2-naphthyl)-1′-propenyl]benzoic acid (Ch80) [100], with a 3′-(1-adamantyl)-4′-[2-(methoxy)ethoxymethoxy]phenyl ring having substituents at its 6′-position [94]. Like MX-781, most of the analogues were able to antagonize the activation of the RAR subtypes by ATRA in a reporter assay. The 6′-hydroxy analogue (**24** in Table **9**) was the most potent antagonist overall, whereas this activity was reduced in alkoxy analogues **11a**–**11j**. Like the 4′-[2-(methoxy)ethoxymethyl] (MEM) ether, MX-781, these ether analogues inhibited ATRA-resistant MDA-MB-468 breast cancer and PC-3 prostate cancer and ATRA-sensitive Jurkat leukemia cell growth in the low μM range (0.4–2.4 μM) and at 2 μM induced Jurkat cell apoptosis (19%–43% after 3 h). However, the cells were grown in medium containing only 0.5% fetal bovine serum. Piedrafita earlier reported that cell growth at low serum levels enhanced the antiproliferative and apoptotic activities of such retinoid-related compounds [101]. At 20 μM, analogues having a 6′-*n*-propyloxy to 6′-*n*-hexyloxy or 6′-benzyloxy group were more effective inhibitors of IKKβ kinase activity (> 80%) than MX-781 (65%).

The de Lera and Peidrafita groups next extended their introduction of 6′-methyl groups to analogues of 5-Cl-AHPN and 3-Cl-AHPC (Table **10**) [93]. The resulting 6′-methyl-4′-hydroxyl and 4′-MEM ether analogues at 4 μM displayed weak RARα antagonism against 20 nM ATRA (4–40%); however, the added 6′-methyl group also induced RXR transcriptional agonism at 2 μM that was most effective in the cinnamic acids **34** and **35** and phenyl acetate **24**. Neither RARα antagonism nor RXR agonism appeared to correspond to caspase activation at 4 h as evidenced by the low caspase-inducing activities of **24** and **34**. In the 6′-methyl-substituted series, at 4 μM the 5-Cl-AHPN analogues were the most potent inhibitors of ATRA-resistant cancer cell growth and the 3-chlorophenylacetates the least potent. Their abilities to inhibit cancer cell growth were assessed on cells grown in 0.5% serum, which would be expected to enhance their efficacy. The susceptibility of the cells in low serum to growth inhibition and apoptosis induction may have been due to higher concentrations of available compound

Table 9. Adamantyl-Substituted Chalcones Inhibit Binding of All-Trans-Retinoic Acid to Retinoic Acid Receptor Subtypes, Cancer Cell Growth, and Activity of the NFκB Kinase IKKβ

Chalcone series	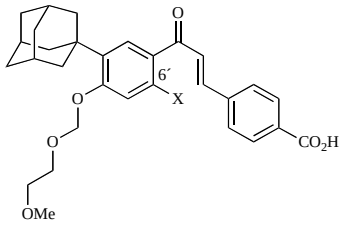	Inhibition of RAR activation by 0.2 μM ATRA by 2 μM cmpd (%)[a]			50% inhibition of cell growth (IC_{50}, μM)[b]			LeuC apoptosis at 2 μM[c]	Inhibition of IKKβ activity at 20 μM[d]
Cmpd No[e]	**X**	**RARα**	**RARβ**	**RARγ**	**BC**	**PC**	**LeuC**	**(%)**	**(%)**
24	OH	71	32	30	6.1	2.5	1.9	21	33
11a	OEt	41	19	20	1.8	1.9	1.1	19	77
11b	O[*n*-$(CH_2)_2CH_3$]	41	17	20	1.4	1.3	0.8	29	82
11c	O[*n*-$(CH_2)_3CH_3$]	26	15	19	0.9	0.7	0.4	45	89
11d	O[*n*-$(CH_2)_4CH_3$]	14	5	19	1.1	1.3	0.5	35	82
11e	O[*n*-$(CH_2)_5CH_3$]	9	9	15	1.9	1.4	0.7	28	83
11g	$OCH_2CH=CH_2$	14	9	30	1.3	1.2	0.8	38	69
11h	OCH_2CCH	35	15	10	1.0	0.8	0.6	43	88
11i	OCH_2Ph	19	14	17	0.9	1.3	0.4	36	79
11j	$OCH_2CH=CHPh$	19	12	16	1.8	2.4	1.0	34	41
Control									
7 (MX-781)	H	60	30	40	2.1	1.5	1.2	19	63

Taken from Ref. [94].

[a]Relative transactivation of Gal4–RAR subtype ligand-binding domains on the UAS–luciferase reporter construct by 0.2 μM all-trans-retinoic acid (ATRA) alone (100%) and in the presence of 2.0 μM compound in transfected CV-1 cells grown in medium containing 5% charcoal-treated fetal bovine serum (FBS). Activation was normalized for transfection efficiency using β-galactosidase activity and determined from graphs presented in Fig. (**2B**) of Ref. [94].

[b]MTT assays on MDA-MB-468 breast cancer (BC), PC-3 prostate cancer (PC), and Jurkat leukemia (LeuC) cells were conducted after treatment for 48 h, 48 h, and 24 h, respectively, in 0.5% FBS-containing medium.

[c]Apoptosis was determined after a 3-h treatment of Jurkat cells, measured by phosphatidylserine externalization, and calculated from graphs shown in Fig. (**4B**).

[d]IKKβ activity relative to control was based on cleavage of [^{32}P]-γ-ATP by baculovirus-expressed $(His)_6$-HA–IKKβ and GST–IKKα and determined from graphical data in Fig. (**5**) of Ref. [94]. Background control contained GST–IKKα.

[e]Compound numbers refer to those in Ref. [94].

when serum binding proteins such as albumin were excluded, the induction of cell stress at reduced levels of growth factors, or the combination.

Pharmacokinetic Studies on AHPC

Analysis of plasma samples from Phase I patients treated with 210 mg of AHPC/ST1926 orally produced at day 2 a maximal concentration (C_{max}) of 529 ± 547 mg/ml and an area-under-the-time-curve (AUC) of 1,133 ± 767 ng/ml h [80]. Thus, peak plasma levels of ST1926 of 1 μM were considered to be achievable [78]. The plasma half-life of ST1926 ranged from 2 to 7 h [80]. At day 2, 80% of the ST1926 dose in the plasma was transformed to glucuronide metabolites as was evidenced by the 8 to18-fold increases in the C_{max} levels of ST1926 and the 9 to 54-fold rise in its AUC values after treatment of the plasma with β-glucuronidase, which cleaves the glucuronide bond.

Mechanistic Studies

The adamantyl-substituted retinoid-related molecule (ARR) AHPN (CD437) was initially reported as a RARγ-selective retinoid with K_D values of 6,500 nM for binding to RARα, 2,400 nM for RARβ, and 77 nM for RARγ [38]. AHPN was found to induce apoptosis in a variety of malignant cell lines including those for breast, lung, ovarian, and prostate cancer, leukemia, and lymphoma [40, 46, 52, 102, 103]. The role, if any, of the RARs in AHPN-mediated apoptosis is at best controversial and may be cell-type specific. Sun *et al.* [63] found that the addition of RARβ/γ-selective retinoids blocked AHPN-mediated growth inhibition of human head-and-neck squamous cell carcinoma cell lines, whereas RAR antagonists had no effect on AHPN-mediated apoptosis in non-small-cell lung cancer and squamous carcinoma cell lines [52, 62]. AHPN-induced apoptosis of neuroblastoma cells was inhibited by approximately 50% by an

Table 10. AHPN and AHPC Analogues Induce Leukemia Cell Apoptosis and Inhibit Cancer Cell Proliferation

5-Cl-AHPN series	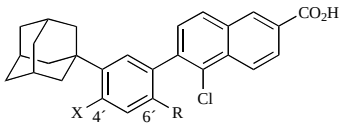		**Relative caspase activity after 4 h**[a]		**Effect (%) on RARα activity by 20 nM ATRA**[b]	**RXRα activity (%)**[c]	**Cancer cell line growth inhibition (%) by 4 μM ARR**[d]			
							48 h		**72 h**	
Cmpd No[e]	**X**	**R**	**1 μM**	**4 μM**	**4 μM**	**2 μM**	**OC**	**PC**	**BC**	**LC**
5 (5-Cl-AHPN)	OH	H	ND[f]	ND						
29	OMEM	Me	1	52	70	29	71	98	50	88
30	OH	Me	21	54	75	4	87	98	59	88
3-Cl-AHPC series	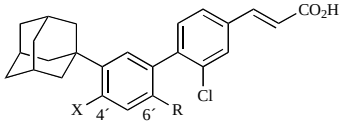									
7 (3-Cl-AHPC)	OH	H	22	ND						
34	OMEM	Me	1	1	73	83	80	72	42	51
35	OH	Me	1	26	96	69	65	69	25	24
3-Cl-Phenyl acetates	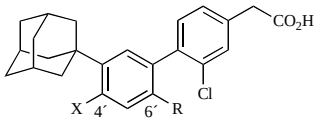									
24	OMEM	Me	0	3.8	60	70	19	52	25	7.9
25	OH	Me	0	29	86	6	30	67	11	16
Controls										
9 (MX781 / CD2674)	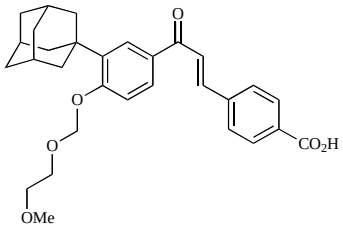		13	41	18		62	92	72	42
2 (CD2325)	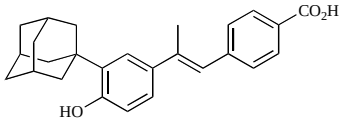		23	49			67	92	77	79
ATRA	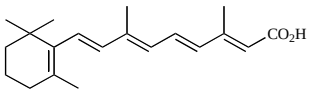				100					
36 (9-cis-RA)	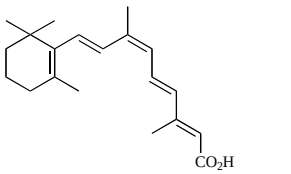					100				

Taken from Ref. [93].

[a]Apoptosis of Jurkat leukemia cells was expressed as increase in DEVDase (caspase) activity induced by 1 μM and 4 μM compound after 4 h with cells grown in presence of 0.5% fetal bovine serum (FBS) and was determined from graphs in Fig. (**3**) of Ref. [93].

[b]Luciferase activity, which was induced by activation of the Gal4–RARα ligand-binding domain (LBD) on the UAS–LUC reporter in CV-1 cells grown in medium containing 0.5% FBS after a 6-h treatment with 20 nM ATRA (100%) alone, or that induced by 20 nM ATRA in the presence of 4 μM compound. Compound-induced increases in activity were determined from graphs in Fig. (**4B**) of Ref. [93]. Only (**2**) had RARα agonist activity at 2 μM (45% that of 1 μM ATRA as 100%).

[c]Luciferase activity was induced by activation of the Gal4–RXRα LBD on the UAS–LUC reporter in CV-1 cells by 2 μM compound after 20 h compared to that by 1 μM 9-cis-RA (100%). Compound-induced increases in activity were determined from graphs in Fig. (5A) of Ref. [93].

[d]Inhibition of PC-3 prostate cancer (PC), SKOV-3 ovarian cancer (OC), MDA-MB-468 breast cancer (BC), and A549 lung cancer (LC) cell proliferation relative to control (≤ 0.1% DMSO) with cells treated in medium containing 0.5% FBS for the specified time, and measured by 3-[4,5-dimethylthiazol-2-yl]-2,5-diphenyltetrazolium bromide (MTT) assays.

[e]Compound numbers were taken from Ref. [93].

[f]ND, not determined.

RARβ/γ-selective antagonist [20]. However, other results did not support a role for the RARs in AHPN-mediated apoptosis. For example, AHPN-mediated apoptosis occurred in the ATRA-resistant HL-60R myeloid leukemia cell line that expresses a truncated version of RARα lacking the terminal 50 amino acids of the wild-type RARα ligand-binding domain, which binds poorly to ATRA, and does not express RARβ or RARγ [44]. Moreover, the AHPN analogue 3-Cl-AHPC, which only binds RARγ but does not transactivate any RAR subtype, is a potent inducer of apoptosis in malignant cells [86]. The inhibition of cell proliferation and induction of apoptosis by these ARRs occured in cancer cell lines that are resistant or refractory to the effects of ATRA and other classic retinoids. Thus, RAR activation by AHPN and its analogues may only be required under specific conditions and with specific cell types.

Nuclear extracts from HL-60R cells displayed specific binding for AHPN [81]. Binding was not competed by either RAR-selective ATRA or RAR and RXR-selective 9-cis-RA to suggest that binding by AHPN was not to either an RAR or RXR [81]. Subsequent studies demonstrated AHPN specifically bound to the nuclear orphan receptor small heterodimer partner (SHP). Binding of AHPN to SHP led to the binding of SHP to the multiprotein repressor complex Sin3A [82, 83]. As a result of SHP binding, the Sin3A complex exhibited an increase in its associated histone deacetylase (HDAC) activity and enhanced binding of HSP90, HDAC4, and the nuclear receptor corepressor NCoR [82, 83]. The 3-Cl-AHPC-enhanced expression of the transcription factors c-Jun and c-Fos was essential for maximal 3-Cl-AHPC-induced apoptosis [83]. Knockdown or knockout of Sin3A or SHP inhibited both 3-Cl-AHPC-induced c-Jun and c-Fos expression and 3-Cl-AHPC-mediated apoptosis [82, 83].

AHPN-mediated apoptosis was found to be preceded by cell-cycle arrest [40, 46, 50, 54, 102, 104-106]. AHPN-associated cell-cycle arrest appeared to involve processes that were distinct from those involved in the induction of apoptosis [54, 98]. Inhibition of AHPN-induced apoptosis by inhibition of caspase or MAPK activation or by an AHPN antagonist such as 3-A-AHPC had no effect on AHPN-mediated cell-cycle arrest [53, 54]. The specific phase of the cell cycle in which arrest occurred appears to be cell-type dependent and most likely secondary to the specific growth-regulatory genes expressed in the cell. The exposure of the MDA-MB-468 breast carcinoma cell line to AHPN resulted in G_0/G_1 arrest [40], whereas, exposure of other malignant cell lines such as those for glioma, melanoma, prostate carcinoma, T-cell lymphoma, and acute myelogenous leukemia, and normal mammary cells resulted in S-phase growth arrest [40, 46, 52, 102, 103]. In several systems, treatment with AHPN was found to enhance the expression of the cyclin-dependent kinase inhibitor $p21^{WAF1/CIP1}$ [40, 46]. Upregulation of $p21^{WAF1/CIP1}$ levels by AHPN occurred through the enhanced stability of $p21^{WAF1/CIP1}$ mRNA levels [40, 42] in the 1.5-kb region of its 3´-UTR [42].

During the apoptotic process induced by a number of agents, the related family of cysteine proteases termed caspases are activated and then cleave proteins after their cysteine–proline peptide sequences [107-109]. Caspases can be activated during either the intrinsic (caspases-9, 3, and 7) or extrinsic (caspases-8 and 10) apoptosis pathways [101]. AHPN treatment resulted in rapid caspase activation [53, 101]. However, caspase activation did not appear to be required for AHPN-induced apoptosis in certain cell types [53]. For example, the pancaspase inhibitor ZVAD-FMK was unable to block AHPN-induced T-cell lymphoma cell death [53].

A plethora of pathways by which AHPN and its analogues induce the apoptosis of malignant cells has been described. Exposure of cells to AHPN was found to activate their ERK, p38, and JNK MAPK pathways [48, 54, 86, 110-112]. Exposure of HL-60R cells to AHPN resulted in the activation of p38 and JNK/SAPK within an hour [48]. While inhibition of p38 activation had no effect on AHPN-induced HL-60R apoptosis and occurred downstream of caspase activation and apoptosis [48], activation of JNK and p38 in human epithelial respiratory cells and ovarian carcinoma cells, respectively, was required [111, 112]. Inhibition of the activation of either kinase by specific inhibitors blocked AHPN-mediated apoptosis in these cells [111, 112]. When human primary acute myelogenous leukemia cells were exposed to 3-Cl-AHPC, the p38, ERK, and JNK kinases were rapidly activated [86]. While inhibition of p38 or ERK activation had no effect on 3-Cl-AHPC-mediated apoptosis, inhibition of JNK activation inhibited apoptosis by approximately 20% to suggest that JNK had a minor role [86]. Exposure of H460, H292, and A549 lung and LNCaP prostate carcinoma cells to either AHPN or 3-Cl-AHPC also resulted in rapid JNK activation, enhanced expression of the orphan nuclear receptor TR3/Nur77/NGFI-B (human, mouse, and rat) or NR4A1 followed by its phosphorylation and subsequent nuclear export [113]. Inhibition of AHPN or 3-Cl-AHPC-induced JNK activation blocked this entire process and apoptosis induction [113]. Binding of Bcl-2 by NR4A1 was shown to convert the function of Bcl-2 from inhibition to enhancing apoptosis [113]. Liang *et al*. [114] reported that exposure of human neuroblastoma and esophageal carcinoma cells to AHPN resulted in the nuclear export and subsequent binding of NR4A1 (TR3) to Bcl-2 located in the ER. The TR3–Bcl-2 interaction resulted in the ER stress response and cell death.

NFκB activation has been associated with inhibition of apoptosis [115-118]. Recent studies have documented that NFκB activation can also play a major role in the induction of apoptosis [119-124]. Exposure of breast and prostate cancer cells to AHPN or 3-Cl-AHPC led to NFκB activation within 24 h [125, 126]. Inhibition of NFκB signaling by dominant-negative IαKβ, p65 knockout, or inhibition of p65 nuclear translocation by helenalin inhibited AHPN or 3-Cl-AHPC-mediated NFκB activation and apoptosis [125, 126]. 3-Cl-AHPC-induced activation of NFκB was associated with the formation of a p65/p50 nuclear complex and enhanced expression of DR4 and DR5 [125, 126]. The combination of the AHPN and TRAIL and the subsequent increase in the binding of TRAIL to DR4 markedly enhanced apoptosis over that noted with either agent alone [126].

AHPN and its analogues have demonstrated activity against a number of tumors in nude mouse xenograft models. AHPN inhibited the growth of human melanoma and ovarian carcinoma cells in nude mice and prolonged their survival

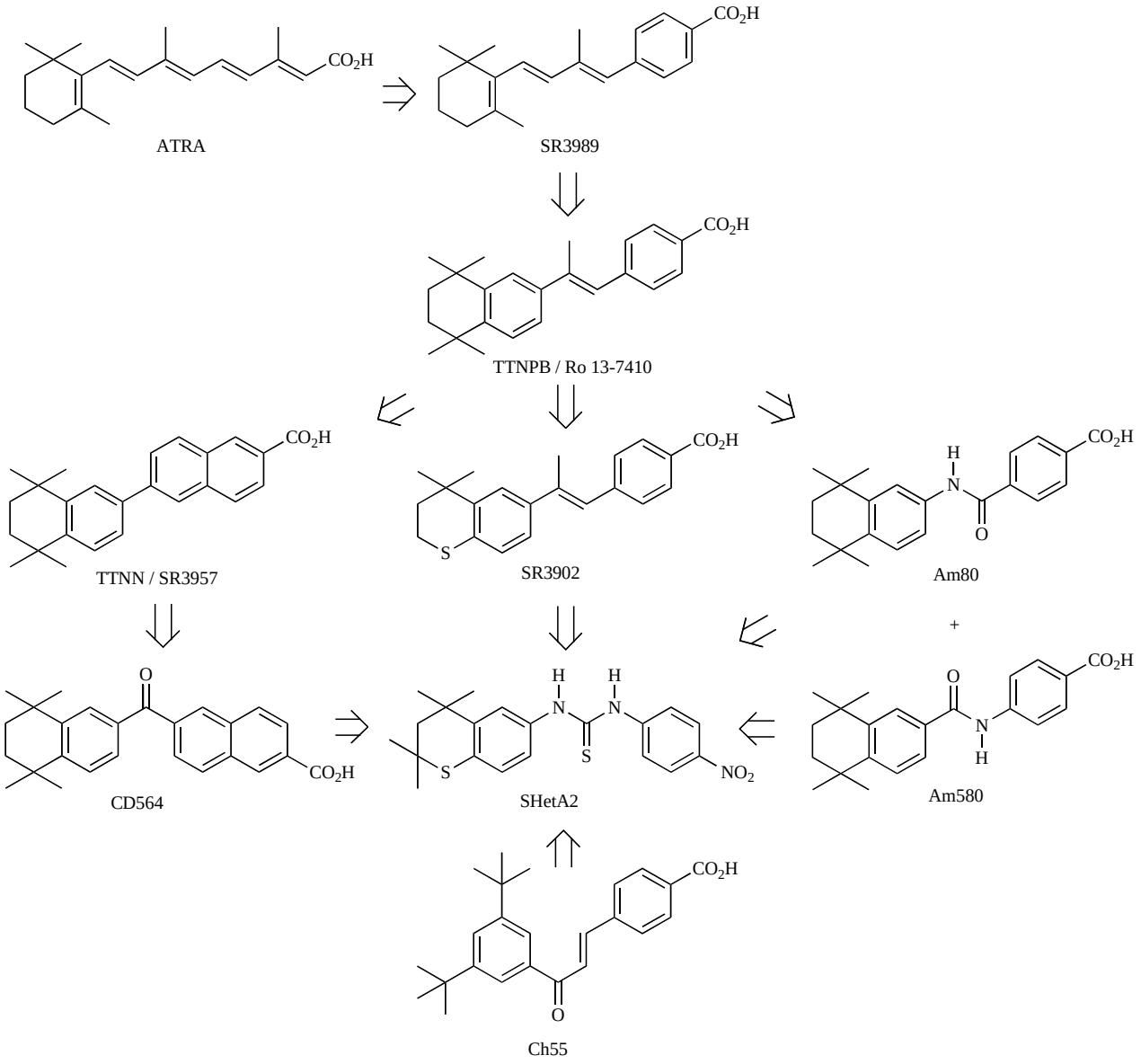

Fig. (3). Probable evolution of the three-atom (thiourea) bridged flexible-heteroarotinoid compounds such as SHetA2 from reported retinoic acid receptor-selective retinoids having a one-atom bridge such as a carbonyl group linking the aromatic ring systems as found in CD564, two-atom bridges such as (*E*)-ethenyl in TTNPB / Ro13-7410 and SR3902, aminocarbonyl as in Am80, and amido as in Am580, and a three-atom bridge such as (*E*)-propenoyl as in Ch55.

[127, 128]. Similar results, namely significant inhibition of tumor growth, were obtained using AHPN analogue MX-3350-1 or MX-781 in nude mice with palpable tumors grown from implanted H292 lung or MDA-MB-468 human breast carcinoma cells, respectively [66, 69].

HETEROAROMATIC RETINOIDS AND UREA AND THIOUREA-BRIDGED ANALOGUES

Overview

On the basis of *in vivo* results and pharmacologic tests, *N*-(2,3-dihydro-2,2,4,4-tetramethyl-6-benzopyranyl),*N′*-(4-nitrophenyl)thiourea (SHetA2 in Fig. (**1**), **15c** in Table **12**) has been projected to enter phase I clinical trials for treatment of ovarian cancer in 2010 [129]. By the time of eventual diagnosis, 5-year survival in ovarian cancer is very low. Dr. Doris M. Benbrook (University of Oklahoma Health Sciences Center, Oklahoma City, OK) has been the driving force in the translational efforts on SHetA2, which was first synthesized by the group of her long-term collaborator, Dr. R. Kenneth Berlin (Oklahoma State University, Stillwater, OK) [130]. The development of SHetA2 has been supported by the U.S. National Cancer Institutes RAPID and RAID programs for new drugs for cancer prevention and treatment, respectively. The probable evolutionary history of these compounds from ATRA is suggested by the structures shown in Fig. (**3**).

Although Dr. Benbrook and collaborators reported that SHetA2 was nonmutagenic in the Ames assay, even on pre-

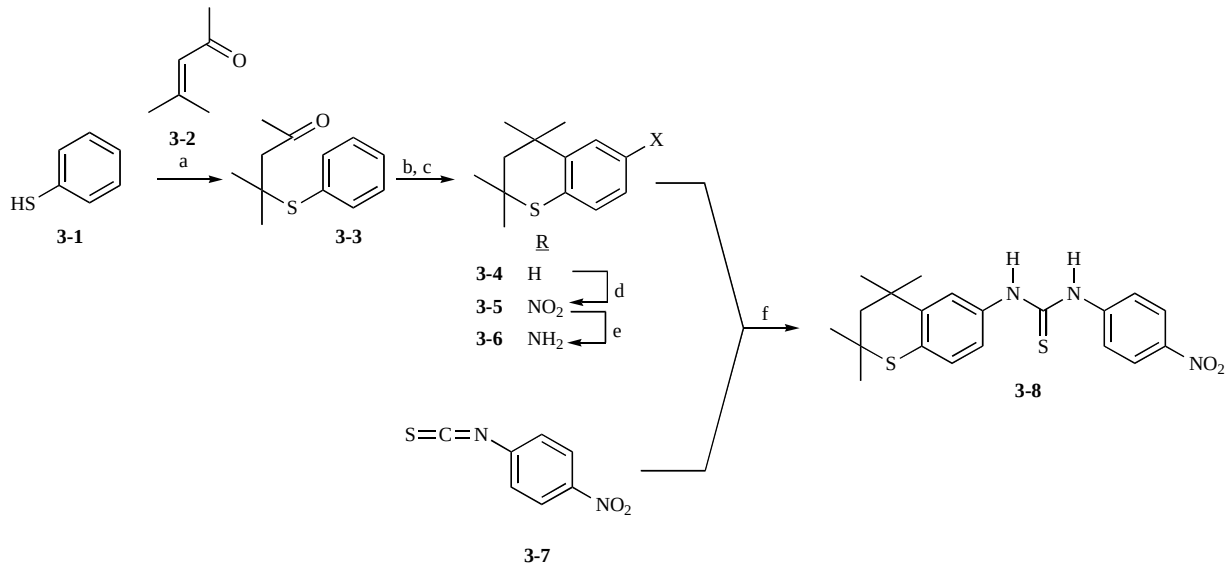

Scheme 3. (a) $HCCl_3$, Et_3N, 0 °C to reflux (77%) [134]. (b) [MeI, Mg, Et_2O]; Et_2O; ice, 5% aq H_2SO_4 (75%) [134]. (c) [$AlCl_3$, CS_2], CS_2, rt to reflux (89%) [134]. (d) HNO_3, Ac_2O, −5 °C; $NaHCO_3$ (26%) [130]. (e) Fe, HOAc, EtOH, reflux (40%) [130]. (f) THF, 0 °C to rt (82%) [130].

incubation with liver microsomes [129], preliminary tests evaluating the metabolites that the gut microflora would produce on oral administration of SHetA2 to patients have not been reported. For example, a potential metabolite could be 4-nitroaniline, which was reported to be a linear mixed inhibitor of tissue kallikrein (K_i = 39 ± 5 μM, K_i' = 298 ± 93 μM) [131] and mutagenic after metabolic activation [132], as well as producing on long-term dosing of rats by gavage methemoglobinemia at 1.5 mg/kg/day and low-level anemia at 9.0 mg/kg/day [133].

Synthesis

The synthetic route to SHetA2 is outlined in Scheme **3**. This synthesis has the advantages of being only six steps in length and using readily available, inexpensive starting materials [130, 134].

Structure–Activity Relationships of Heteroarotinoids

The first heteroaromatic retinoid analogues investigated by the collaborating Benbrook and Berlin groups were heterocyclic analogues of (*E*)-4′-[2-(5,6,7,8-tetrahydro-5,5,8,8-tetramethyl-2-naphthyl)propenyl]benzoic acid (TTNPB, Ro13-7410) (Table **11**) [134-136]. The majority of these analogues had a dihydrobenzopyran ring, an ester bridge between the two aromatic rings, and a carboxylate ester terminus. The ester bridge might be expected to have limited half-life *in vivo*. The most comprehensive screening on this group of analogues (**5**–**19** in Table **11**) was conducted against the growth of two head-and-neck cancer cell lines [135]. Analogue **16** having an aminocarbonyl bridge linking the dihydrobenzothiopyran and benzoate rings was the most active at 10 μM (37–64% growth inhibition) followed by ester-bridged dihydropyran **10** (6–52%). The tetrahydroquinolines **17**–**19** were poor inhibitors (5–25%) [135, 136]. Higher growth inhibitory potencies for **17**–**19** were observed against cervical and vulvar cancer cell growth (13–40% and 25–84%, respectively).

The sulfur and oxygen-containing heteroarotinoids having an (*E*)-2-methylethenyl bridge were evaluated for retinoid activity in the vitamin A-deficient tracheal organ culture reversal of keratinization assay (TOC assay) and in the mouse epidermal ornithine decarboxylase activity inhibition assay (ODC assay), in which 12-*O*-tetradecanoylphorbol-13-acetate (TPA) was used to induce ODC. The carboxylic acids (**1d**/**13***** and **14*****) proved to be more active than their ethyl esters (**1c** and **1b**) in the TOC assay [137, 138] but less potent than ATRA. In the ODC assay, at the 1.7-nmole topical dose the carboxylic acids **1d**/**13***** and **14***** inhibited enzyme activity by 42% and 68%, respectively, whereas ATRA inhibited activity by 88% [137]. In the two-stage tumor promotion assay in which female mice were initiated with topical DMBA and then promoted with topical TPA for 20 weeks, at the topical dose of 17 nmoles **14***** was more effective at decreasing the average number of papillomas per mouse (93 ± 2% decrease) than **13***** (75 ± 1%) or ATRA (74 ± 1%). A maximum-tolerated dose study in female mice indicated that **14***** was less toxic than **13*****, which was less toxic than ATRA [137].

The heteroaromatic retinoids containing three-atom urea and thiourea bridges between the aromatic rings were termed flexible heteroarotinoids (flex-hets) by the Benbrook group [139]. Comparison of the growth inhibitory activities of the dihydrobenzothiopyranyl thiourea and urea flex-hets against renal and ovarian cancer cell lines compared to normal renal and endometrial cells suggested a 1.5 to 2-fold difference at most in preferential potency against the cancer cell lines. When evaluated at 10 μM, SHetA2 (**15c** in Table **12**) and SHetC2 (**10c**), which were terminated by 4-nitrophenyl groups were more potent inhibitors of the growth of the two renal cancer lines than SHetA3 (**15b**) and SHetA4 (**15a**), which were terminated by 4-carbethoxy groups [139]. SHetA2 was also more active than SHetA3 or SHetA4 in

Table 11. Heteroaromatic Retinoids and Their Effects on Proliferation of Cancer Cell Lines in Culture and Reversal of Keratinization in Vitamin A-Deficient Hamster Trachea in Organ Culture

TTNBP series	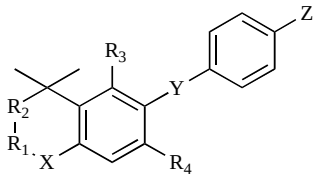							Cancer cell line growth inhibition at 10 μM for 72 h (%)								Relative TOC activity[e,f]
								CC[a]		H&N[b,c]		OC[d]		VC[d]		
Cmpd No[g]	X	R_1	R_2	R_3	R_4	Y	Z	1	2	1	2	1	2	1	2	Ratio
5	O	CH_2	CH_2	H	H	CO_2	CO_2Et			–6	13					
6 (OHet72)	O	CH_2	CH_2	H	H	CO_2	$CNNHC(S)NH_2$			19	18					
7	O	CH_2	CH_2	H	H	CONOMe	CO_2Me			3	17					
8	O	CMe	CH	Me	Me	OCO	CO_2Me			15	–8					
9	O	CMe_2	CH_2	Me	Me	OCO	CO_2Me			–1	9					
10	CMe_2	CH_2	O	H	OMe	CO_2	CO_2Et			52	6					
11 (Arot21)	CMe_2	CH_2	CH_2	H	OMe	CO_2	CO_2Et			15	12					
12	O	CH_2		H	H	*E*-MeC=CH	CO_2H			1	1					
16 (SHet50)	S	CMe_2	CH_2	H	H	NHCO	CO_2Me			64	37					
17/1* (NHet86)	MeN	CH_2	CH_2	H	H	CO_2	CO_2Et	40*	25*	12 19*	13 19*	0	1	34	14	
18/2* (NHet90)	MeN	CH_2	CH_2	H	Me	CO_2	CO_2Et	26*	16*	9 19*	7 17*	5	0	81	84	
19/3* (NHet17)	*i*-PrN	CH_2	CH_2	H	H	CO_2	CO_2Et	25*	13*	5 22*	15 25*	6	2	47	25	
1b	S	CH_2	CH_2	H	H	*E*-MeC=CH	CO_2Et									3
14***	S	CH_2	CH_2	H	H	*E*-MeC=CH	CO_2H									5***
1c	O	CH_2	CH_2	H	H	*E*-MeC=CH	CO_2Et									11
1d/13***	O	CH_2	CH_2	H	H	*E*-MeC=CH	CO_2H									60 20***
1e	SO	CH_2	CH_2	H	H	*E*-MeC=CH	CO_2Et									10
15	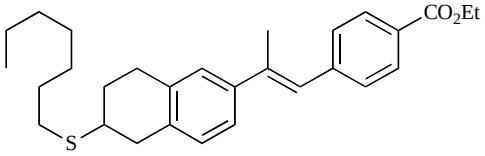									10	17					
ATRA series	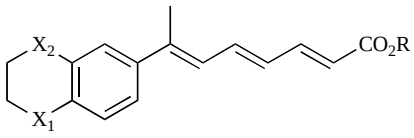															

(Table 11). Contd…..

Cmpd No	X_1	X_2	R										
13	O	O	Et				–33	–2					
14	S	CMe_2	H				2	1					
Controls													
TTNPB	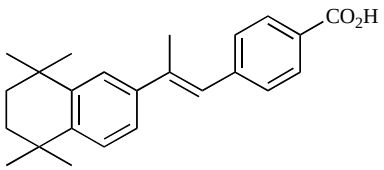								11	19	34	19	
9-cis-RA	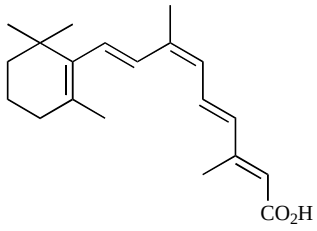				25*	13*	13 25* 49**	10 23*	25	31	38	31	
4-HPR	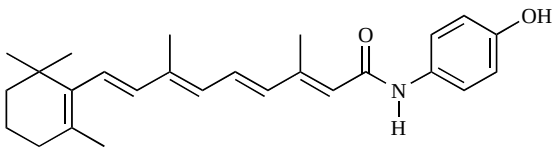						74**						

Taken from Ref. [135-138, 140].

[a–d]Growth inhibition (%) induced by 10 μM heteraromatic retinoid after 72 h in [a]SiHa and CC-1 cervical cancer cells (CC 1 and 2, respectively) [136]; [b,c]SCC-2 [136] and SCC-38 [135] head-and-neck squamous carcinoma cells (H&N 1 and 2, respectively); [d]CAOV-3 (OV 1) and SKOV-3 (OV 2) ovarian cancer cells, and SW954 (VC 1) and SW962 (VC 2) vulvar cancer cells [136] was determined spectrophotometrically after sulforhodamine B staining. H&N data that is not superscripted refers to Ref. [135], that labeled with one asterisk refers to Ref. [136] and was taken from graphical data in Fig. (1) of Ref. [136], and that labeled with two asterisks refers to Ref. [140] and was taken from graphical data in Fig. (2) of Ref. [140].

[e]TOC, relative activity expressed as ratio of ED_{50} value of a heteroarotinoid to that of ATRA (EC_{50} normalized to 1×10^{-11} M) required to reverse keratinization by 50% in vitamin A-deficient hamster trachea in organ culture [138].

[f]Data and compound numbers labeled with three asterisks taken from Ref. [137].

[g]Compound numbers **5**–**19** and **1b**–**1e** refer to those cited in Ref. [135] and [138], respectfully.

inhibiting the growth of three ovarian cancer cell lines and four cervical cancer cell lines [130, 139]. SHetA2 and SHetC2 did not transactivate the RARs at 10 μM [140].

Pharmacokinetic Studies

The ability of SHetA2 to inhibit the growth of ovarian, lung, and head-and-neck carcinoma cells in xenograft models [139, 141, 142] led to pharmacokinetic studies in the mouse. The oral bioavailability of SHetA2 in the mouse was 15% at 20 mg/kg and 19% at 60 mg/kg [143]. An intravenous 20-mg/kg dose of SHetA2 to mice produced a plasma concentration of 10 μM after 5 min, which then declined biexponentially. Following oral administration of SHetA2, maximal mean plasma concentrations in the mouse were found to be 0.79 μM and 2.35 μM at 2 h and 3 h, respectively. In human plasma SHetA2 was found to be 99.3–99.5% protein bound and its stability (half-life) was approximately 50% at 12 h.

Mechanism of Action Studies on SHetA2

The heteroarotinoids represent a novel class of molecules that have been demonstrated to inhibit the growth of a number of malignant cell types both *in vitro* and *in vivo*. These compounds modulate a number of cellular processes that may contribute to their ability to induce apoptosis of malignant cells [140]. The synthetic flexible heteroarotinoids (flex-hets) appear to induce apoptosis through RAR and RXR-independent pathways. These compounds neither bind nor activate the RARs or RXRs [140]. Their ability to induce apoptosis in squamous carcinoma cell lines was documented by the use of Tunel assays and annexin V binding as assessed by flow-cytometry. Exposure of squamous carcinoma cells to the flex-het SHetA2 resulted in the generation of ROS. Inhibition of ROS generation utilizing a number of radical scavengers resulted in a decrease in SHetA2-mediated apoptosis [140]. Later studies were more consistent with the fact that ROS generation was more a consequence of apoptosis induction rather than the cause of apoptosis. Exposure of the CaOV-3, OVCAR-3, and SK-OV-3 ovarian carcinoma cell lines to SHetA2 led to the induction of apoptosis (EC_{50} values ranging from 0.9 to 10 μM) [130].

The ability of SHetA2 to specifically target the mitochondria in malignant cells rather than in normal cells was documented. Exposure of squamous carcinoma cells to SHetA2 for a little as 30 minutes resulted in a decrease in mitochondrial permeability transition as measured by 3,3´-dihexyoxacarbocyanine iodide uptake [140]. The SHetA2-mediated decrease in mitochondrial permeability transition was followed very quickly by the release of mitochondrial

Table 12. Flexible Heteroaromatic Retinoids Having Three-Atom Thiourea and Urea Bridges between the Aromatic Rings and Their Effects on Cancer Cell Growth

Benzo-thiopyran series	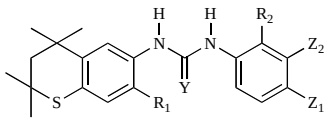					Cell growth inhibition													
						RC (%)[a]		RN (%)[a]		OC (%)[b]			EC_{50} (μM)[c]		CC (%)[d]				H&N(%)[d]
Cmpd No[e]	Y	Z_1	Z_2	R_1	R_2	1	2	1	2	1	2	3	OC 4	NE	1	2	3	4	
15c / 10a (SHetA2)	S	NO_2	H	H	H	84	72	51	37	55	67	45	1.7	3.0	68	58	87	92	81
15b / 10b (SHetA3)	S	CO_2Et	H	H	H	56	54	35	28	24	58	42	2.9	2.7	58	42	84	65	39
15a / 10d (SHetA4)	O	CO_2Et	H	H	H	69	45	26	40	40	69	47	2.8	4.5	67	59	85	76	42
10c (SHetC2)	O	NO_2	H	H	H	86	79	53	52				1.0	2.3					
(SHetD3)	O	CO_2Me	H	H	H	57	62	26	46										
(SHetD4)	S	CO_2Me	H	H	H	39	45	44	38										
(SHetD5)	S	H	CO_2Me	H	H	34	42	48	ND[f]										
15e (SHetA19)	S	NO_2	H	H	Me					32	65	51							68
15d	S	SO_2NH_2	H	H	H					11	32	33							
15f	O	CO_2Et	H	Me	H					34	46	49							
15g	O	CO_2Et	H	Me	H					23	49	55							
15h	S	SO_2NH_2	H	Me	H					19	39	44							
Quinoline series	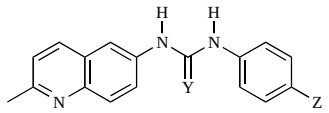																		
Cmpd No	**Y**		**Z**																
9a	S		NO_2										5.0	>1,000					
9b	O		NO_2										7.9	>1,000					
9c	O		CO_2Et										4.9	>1,000					
Control																			
ATRA	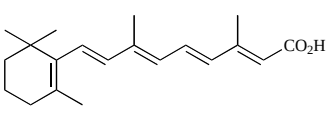					6.5	0	16	ND										52

(Table 12). Contd…..

9-cis-RA	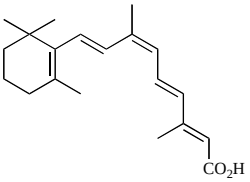									>10	24	28	45	47	51
25 (4-HPR)	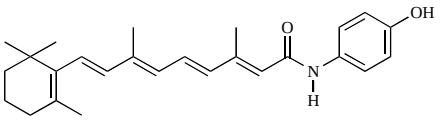					62	43	65		>10					74

Taken from Ref. [130, 139, 140, 147, 148].

Growth inhibition (%) by 10 μM compound after 48 h on the following cell lines:

[a]Caki-1 (RC 1) and 786-0 (RC 2) renal cancer cells and HK-2 (RN 1) and RTC91696 (RN 2) normal human kidney cells treated with 12.5 μM being the highest concentration evaluated [147];

[b]CAOV-3 (OC 1), OVCAR-3 (OC 2), and SKOV-3 (OC 3) ovarian cancer cells after treatment for 72 h, which was determined from data in Table 2 of Ref. [130].

[c]EC_{50} values for 50% growth inhibition of A2780 ovarian cancer cells (OC 4) and normal endometrial cells (NE) treated by compounds for 48 h [130, 148].

[d]Growth inhibition (%) of SiHa (CC 1), CC-1 (CC 2), C33a (CC 3), and HT-3 (CC 4) cervical cancer cells [139] and UMSCC38 head-and-neck squamous cell cancer cells (H&N) [140] treated by 10 μM compound for 72 h.

[e]Compound numbers **15a**-**15h** refer to those in Ref. [130], and **9a**–**9c** and **10a**–**10c** refer to Ref. [148].

[f]ND, not determined.

cytochrome *c* into the cytoplasm, activation of caspase-3, and the induction of apoptosis. The ability of SHetA2 to directly effect mitochondrial structure was confirmed in a study by Liu *et al.* [144], in which the Benbrook group examined the ability of the flexible heterocyclic compounds to induce apoptosis in malignant and nonmalignant ovarian cells. These investigators found that exposure of the ovarian cancer cells to 10 μM SHetA2 resulted in marked mitochondrial swelling and loss of mitochondrial integrity. Interestingly, no such effects were seen in normal human ovarian epithelial cells obtained from patients. That SHetA2-mediated mitochondrial swelling occurred in the presence of cycloheximide suggested that protein synthesis was not required for the effect of SHetA2 on mitochondrial structure [144]. This effect of SHetA2 was not dependent on the generation of ROS [144]. SHetA2-mediated mitochondrial swelling was preceded by decreases in Bcl-2 and Bcl-X_L levels. Whether the decreased expression of these two anti-apoptotic proteins was required for mitochondrial swelling to occur remains to be determined. Exposure of normal ovarian or endometrial cells to SHetA2 did not induce any such modulation of mitochondrial structure or protein expression, although these cells did exhibit increases in Bcl-2 and Bcl-X_L levels [144]. Because both proteins have been associated with cytoprotective (anti-apototic) effects, their increased expression may indeed block SHetA2-mediated mitochondrial permeability changes and subsequent apoptosis in normal cells [144].

Exposure of NSCLC cells to SHetA2 also resulted in the induction of apoptosis [141]. Apoptosis induction was preceded by activation of the extrinsic apoptotic pathway involving caspase-8 and DR5 [141]. Expression of caspase-8 silencing RNA blocked SHetA2-mediated apoptosis in the A549 lung carcinoma cell line. Exposure of a number of such lung carcinoma cell lines to SHetA2 also resulted in the expression of DR5 on their cell surface, but DR4 levels were not modulated. Cotreatment of A549, H157, H1299, and Colo-1 cancer cell lines with SHetA2 and TRAIL, which is known to bind and activate DR5, enhanced the number of apoptotic cells over that noted when SHetA2 and TRAIL were added alone. The Sun group also found that SHetA2 enhanced DR5 expression through the enhanced binding of the CAAT/enhancer-binding protein homologous protein (CHOP) to its binding site located in the 5′-flanking region of the DR5 gene. The observation that silencing of DR5 blocked SHetA2-mediated apoptosis suggested that DR5 plays an important role in SHetA2-meditated apoptosis in general [141]. The finding that CHOP is highly inducible during the ER stress process further suggested that SHetA2 may act in cells as an inducer of ER stress. These authors found that SHetA2-exposed A549 and H157 lung cancer cell lines did indeed show increased levels of several proteins associated with ER stress, including Bip/GRP78, IRE1α, ATF4, and XBP-1 [141].

SHetA2 treatment of A2780 ovarian carcinoma cells in organotypic culture resulted in the modulation of a number of genes as demonstrated by utilizing microarrays [142]. Thrombospondin 4 and thymidine phosphorylase were significantly repressed at both the mRNA and the protein levels [142]. Thrombospondin 4 has been found to be angiogenic. Thymidine phosphorylase has also been found to be angiogenic through its ability to convert thymidine to thymine and 2-deoxy-D-ribose 1-phosphate. The latter and its metabolite, 2-deoxy-D-ribose, were found to be angiogenic [142]. SHetA2 inhibited the secretion of vascular endothelial growth factor but enhanced that of basic fibroblast growth factor [142]. The addition of conditioned media from a number of SHetA2-treated malignant cell lines to human umbilical vascular endothelial cells (HUVECs) resulted in a decrease in endothelial tube formation, thus demonstrating the antiangiogenic properties of the proteins secreted into conditioned media following exposure of cancer cells to SHetA2 [142]. Tumors obtained from mice treated with SHetA2 revealed marked disorganization of their vasculature in comparison to tumors obtained from untreated mice. Moreover, tumors obtained from the SHetA2-treated mice displayed an increased number of areas in which blood vessels were absent and necrosis was found [142].

CONCLUSIONS

This review has summarized the discovery and development of three novel classes of retinoid-derived small molecules that were subsequently found to function independently of the retinoid nuclear receptors. Their initial targets remain to be discovered except for the adamantyl-substituted retinoid-related molecules derived from the anti-acne drug adapalene. They interact with the small heterodimer partner nuclear receptor that functions as a transcriptional corepressor of many other steroid/thyroid hormone nuclear receptor family members. However, other signaling pathways such as those leading to cell-cycle arrest and DNA damage also appear involved in its anticancer effects. The initial targets of the peptidomimetic analogues of 4-HPR and flex-hets remain to be established. Members of these three new classes offer exciting opportunities for probing cellular stress responses, mitochondria–endoplasmic recticulum crosstalk, and pathways leading to apoptosis induction. Most important, they exhibit robust potential for cancer treatment and/or prevention.

ACKNOWLEDGEMENTS

Support for the research of the Fontana and Dawson groups on AHPN, AHPC, and their analogues by the U.S. National Cancer Institute, U.S. Veterans Administration, and the California Tobacco-Related Diseases Research Program is gratefully acknowledged.

ABBREVIATIONS

3-A-AHPC = (*E*)-4-[3′-(1-adamantyl)-4′-hydroxyphenyl]-3-(3-acetamidopropyloxy)cinnamic acid

3-Cl-AHPC = (*E*)-4-[3′-(1-adamantyl)-4′-hydroxyphenyl]-3-chlorocinnamic acid

4-HBR = 4-(trans-retinoylmethyl)phenol

4-HBRCG = 2,6-anhydro-7-deoxy-7-[4-(retinoylmethyl)phenyl]-L-glycero-L-guloheptinoic acid

4-HPR = *N*-(4-hydroxyphenyl) trans-retinamide

4-HPRCG = 2,6-anhydro-7-deoxy-7-[4-(retinamido)phenyl]-L-glycero-L-guloheptinoic acid

4-HPROG = 4-HPR-*O*-glucuronide

4-MPR = *N*-(4-methoxyphenyl) trans-retinamide

5-Cl-AHPN = 6-[3′-(1-adamantyl)-4′-hydroxyphenyl]-5-chloro-2-naphthalenecarboxylic acid

9-BBN = 9-borabicyclo[3.3.1]nonane

Ad = adamantyl

AHPC = (*E*)-4-[3′-(1-adamantyl)-4′-hydroxyphenyl]cinnamic acid

AHPN = 6-[3′-(1-adamantyl)-4′-hydroxyphenyl]-2-naphthalenecarboxylic acid

aq = aqueous

ATRA = all-trans-retinoic acid

CAT = chloramphenicol acetyl transferase

CHOP = CCAAT enhancer-binding protein homologous protein

dil = dilute

DMBA = 7,12-dimethylbenzo[*a*]anthracene

DME = dimethoxyethane

DR = death receptor

ER = endoplasmic reticulum

(g) = gas

GADD = growth arrest and DNA-damage gene

HSP = heat shock protein

LUC = luciferase

NSCLC = non-small-cell lung cancer

ODC = ornithine decarboxylase

RAR = retinoic acid receptor

RARE = retinoic acid response element

rt = room temperature

RXR = retinoid X receptor

SHetA2 = [(4-nitrophenyl)amino][(2,2,4,4-tetramethylthiochroman-6-yl)amino]methane-1-thione or *N*-(2,3-dihydro-2,2,4,4-tetramethyl-6-benzothiopyranyl),*N*′-(4-nitrophenyl)thiourea

THF = tetrahydrofuran

TOC = tracheal organ culture

TPA = 12-*O*-tetradecanoyl-13-phorbol acetate

TRAIL = tumor factor-related apoptosis-inducing ligand

TTNN = 6-(5,6,7,8-tetrahydro-5,5,8,8-tetramethyl-2-naphthyl)-2-naphthalenecarboxylic acid

TTNPB = (*E*)-4-[2′-(5,6,7,8-tetrahydro-5,5,8,8-tetramethyl-2′-naphthyl)propenyl]benzoic acid

UPR = unfolded protein response

UTR = untranslated region

REFERENCES

[1] Alshafie, G. A.; Walker, J. R.; Curley, R. W., Jr.; Clagett-Dame, M.; Highland, M. A.; Nieves, N. J.; Stonerock, L. A.; Abou-Issa, H. Inhibition of mammary tumor growth by a novel nontoxic retinoid: Chemotherapeutic evaluation of a C-linked analog of 4-HPR-glucuronide. *Anticancer Res.*, **2005**, *25*, 2391-2398.

[2] Walker, J. R.; Alshafie, G.; Abou-Issa, H.; Curley, R. W., Jr. An improved synthesis of the C-linked glucuronide of *N*-(4-hydroxyphenyl)retinamide. *Bioorg. Med. Chem. Lett.*, **2002**, *12*, 2447-2450.

[3] Weiss, K. L.; Alshafie, G.; Chapman, J. S.; Mershon, S. M.; Abou-Issa, H.; Clagett-Dame, M.; Curley, R. W., Jr. An unhydrolyzable analogue of *N*-(4-hydroxyphenyl)retinamide. Synthesis and preliminary biological studies. *Bioorg. Med. Chem. Lett.*, **2001**, *11*, 1583-1586.

[4] Walker, J. R.; Alshafie, G.; Nieves, N.; Ahrens, J.; Clagett-Dame, M.; Abou-Issa, H.; Curley, R. W., Jr. Synthesis and preliminary chemotherapeutic evaluation of the fully C-linked glucuronide of *N*-(4-hydroxyphenyl)retinamide. *Bioorg. Med. Chem.*, **2006**, *14*, 3038-3048.

[5] Abou-Issa, H.; Curley, R. W., Jr.; Alshafie, G. A.; Weiss, K. L.; Clagett-Dame, M.; Chapman, J. S.; Mershon, S. M. Chemotherapeutic evaluation of 4-hydroxybenzylretinone (4-HBR), a nonhydrolyzable C-linked analog of *N*-(4-hydroxyphenyl) retinamide (4-HPR) against mammary carcinogenesis. *Anticancer Res.*, **2001**, *21*, 3839-3844.

[6] Swanson, B. N.; Newton, D. L.; Roller, P. P.; Sporn, M. B. Biotransformation and biological activity of *N*-(4-hydroxyphenyl) retinamide derivatives in rodents. *J. Pharmacol. Exp. Ther.*, **1981**, *219*, 632-637.

[7] Abou-Issa, H.; Curley, R. W., Jr.; Panigot, M. J.; Wilcox, K. A.; Webb, T. E. *In vivo* use of *N*-(4-hydroxyphenyl retinamide)-*O*-glucuronide as a breast cancer chemopreventive agent. *Anticancer Res.*, **1993**, *13*, 1431-1436.

[8] Dawson, M. I.; Hobbs, P. D. Synthesis of the D-glucuronic acid conjugates of *N*-(4-hydroxyphenyl)- and *N*-(2-hydroxyethyl)-retinamides. *Carbohydr. Res.*, **1980**, *85*, 121-129.

[9] Mershon, S. M.; Anding, A. L.; Chapman, J. S.; Clagett-Dame, M.; Stonerock, L. A.; Curley, R. W., Jr. Solid phase-assisted synthesis and screening of a small library of *N*-(4-hydroxyphenyl)retinamide (4-HPR) analogs. *Bioorg. Med. Chem. Lett.*, **2007**, *17*, 836-840.

[10] Su, B.; Mershon, S. M.; Stonerock, L. A.; Curley, R. W., Jr.; Brueggemeier, R. W. 4-Hydroxyphenylretinamide (4HPR) derivatives regulate aromatase activity and expression in breast cancer cells. *J. Steroid Biochem. Mol. Biol.*, **2008**, *109*, 40-46.

[11] Das, B. C.; Smith, M. E.; Kalpana, G. V. Design and synthesis of 4-HPR derivatives for rhabdoid tumors. *Bioorg. Med. Chem. Lett.*, **2008**, *18*, 3805-3808.

[12] Thatcher, J. E.; Isoherranen, N. The role of CYP26 enzymes in retinoic acid clearance. *Expert Opin. Drug Metab. Toxicol.*, **2009**, *5*, 875-886.

[13] Winum, J. Y.; Leydet, A.; Seman, M.; Montero, J. L. Synthesis and biological activity of glycosyl conjugates of *N*-(4-hydroxyphenyl) retinamide. *Farmaco*, **2001**, *56*, 319-324.

[14] Curley, R. W., Jr.; Abou-Issa, H.; Panigot, M. J.; Repa, J. J.; Clagett-Dame, M.; Alshafie, G. Chemopreventive activities of C-glucuronide/glycoside analogs of retinoid-*O*-glucuronides against breast cancer development and growth. *Anticancer Res.*, **1996**, *16*, 757-763.

[15] Abou-Issa, H. M.; Alshafie, G. A.; Curley, R. W., Jr.; Wong, M. F.; Clagett-Dame, M.; Repa, J. J.; Sikri, V. Chemopreventive activity of a C-glucuronide analog of *N*-(4-hydroxyphenyl) retinamide-*O*-glucuronide against mammary tumor development and growth. *Anticancer Res.*, **1999**, *19*, 999-1004.

[16] Anding, A. L.; Chapman, J. S.; Barnett, D. W.; Curley, R. W., Jr.; Clagett-Dame, M. The unhydrolyzable fenretinide analogue 4-hydroxybenzylretinone induces the proapoptotic genes *GADD153 (CHOP)* and *Bcl-2-binding component 3 (PUMA)* and apoptosis that is caspase-dependent and independent of the retinoic acid receptor. *Cancer Res.*, **2007**, *67*, 6270-6277.

[17] Bonanni, B.; Lazzeroni, M.; Veronesi, U. Synthetic retinoid fenretinide in breast cancer chemoprevention. *Expert Rev. Anticancer Ther.*, **2007**, *7*, 423-432.

[18] Sheikh, M. S.; Shao, Z. M.; Li, X. S.; Ordonez, J. V.; Conley, B. A.; Wu, S.; Dawson, M. I.; Han, Q. X.; Chao, W. R.; Quick, T.; Niles, R. M.; Fontana, J. A. *N*-(4-Hydroxyphenyl)retinamide (4-HPR)-mediated biological actions involve retinoid receptor-independent pathways in human breast carcinoma. *Carcinogenesis*, **1995**, *16*, 2477-2486.

[19] Fanjul, A. N.; Delia, D.; Pierotti, M. A.; Rideout, D.; Yu, J. Q.; Pfahl, M. 4-Hydroxyphenyl retinamide is a highly selective activator of retinoid receptors. *J. Biol. Chem.*, **1996**, *271*, 22441-22446.

[20] Lovat, P. E.; Ranalli, M.; Bernassola, F.; Tilby, M.; Malcolm, A. J.; Pearson, A. D.; Piacentini, M.; Melino, G.; Redfern, C. P. Distinct properties of fenretinide and CD437 lead to synergistic responses with chemotherapeutic reagents. *Med. Pediatr. Oncol.*, **2000**, *35*, 663-668.

[21] Clifford, J. L.; Menter, D. G.; Wang, M.; Lotan, R.; Lippman, S. M. Retinoid receptor-dependent and -independent effects of *N*-(4-hydroxyphenyl)retinamide in F9 embryonal carcinoma cells. *Cancer Res.*, **1999**, *59*, 14-18.

[22] Hail, N., Jr.; Lotan, R. Mitochondrial permeability transition is a central coordinating event in *N*-(4-hydroxyphenyl)retinamide-induced apoptosis. *Cancer Epidemiol. Biomarkers Prev.*, **2000**, *9*, 1293-1301.

[23] Hail, N., Jr.; Lotan, R. Mitochondrial respiration is uniquely associated with the prooxidant and apoptotic effects of *N*-(4-hydroxyphenyl)retinamide. *J. Biol. Chem.*, **2001**, *276*, 45614-45621.

[24] Asumendi, A.; Morales, M. C.; Alvarez, A.; Arechaga, J.; Pérez-Yarza, G. Implication of mitochondria-derived ROS and cardiolipin peroxidation in *N*-(4-hydroxyphenyl)retinamide-induced apoptosis. *Br. J. Cancer*, **2002**, *86*, 1951-1956.

[25] Kim, H. J.; Chakravarti, N.; Oridate, N.; Choe, C.; Claret, F. X.; Lotan, R. *N*-(4-Hydroxyphenyl)retinamide-induced apoptosis triggered by reactive oxygen species is mediated by activation of MAPKs in head and neck squamous carcinoma cells. *Oncogene*, **2006**, *25*, 2785-2794.

[26] Kouhara, J.; Yoshida, T.; Nakata, S.; Horinaka, M.; Wakada, M.; Ueda, Y.; Yamagishi, H.; Sakai, T. Fenretinide up-regulates DR5/TRAIL-R2 expression *via* the induction of the transcription factor CHOP and combined treatment with fenretinide and TRAIL induces synergistic apoptosis in colon cancer cell lines. *Int. J. Oncol.*, **2007**, *30*, 679-687.

[27] Lai, W. L.; Wong, N. S. ROS mediates 4HPR-induced posttranscriptional expression of the Gadd153 gene. *Free Radic. Biol. Med.*, **2005**, *38*, 1585-1593.

[28] Xia, Y.; Wong, N. S.; Fong, W. F.; Tideman, H. Upregulation of GADD153 expression in the apoptotic signaling of *N*-(4-hydroxyphenyl)retinamide (4HPR). *Int. J. Cancer*, **2002**, *102*, 7-14.

[29] Schroder, M. Endoplasmic reticulum stress responses. *Cell Mol. Life Sci.*, **2008**, *65*, 862-894.

[30] Kadara, H.; Lacroix, L.; Lotan, D.; Lotan, R. Induction of endoplasmic reticulum stress by the pro-apoptotic retinoid *N*-(4-hydroxyphenyl)retinamide *via* a reactive oxygen species-dependent mechanism in human head and neck cancer cells. *Cancer Biol. Ther.*, **2007**, *6*, 705-711.

[31] Appierto, V.; Tiberio, P.; Villani, M. G.; Cavadini, E.; Formelli, F. PLAB induction in fenretinide-induced apoptosis of ovarian cancer cells occurs *via* a ROS-dependent mechanism involving ER stress and JNK activation. *Carcinogenesis*, **2009**, *30*, 824-831.

[32] Rehman, F.; Shanmugasundaram, P.; Schrey, M. P. Fenretinide stimulates redox-sensitive ceramide production in breast cancer cells: Potential role in drug-induced cytotoxicity. *Br. J. Cancer*, **2004**, *91*, 1821-1828.

[33] Vené, R.; Arena, G.; Poggi, A.; D'Arrigo, C.; Mormino, M.; Noonan, D. M.; Albini, A.; Tosetti, F. Novel cell death pathways induced by *N*-(4-hydroxyphenyl)retinamide: Therapeutic implications. *Mol. Cancer Ther.*, **2007**, *6*, 286-298.

[34] Ferrari, N.; Pfeffer, U.; Dell'Eva, R.; Ambrosini, C.; Noonan, D. M.; Albini, A. The transforming growth factor-β family members bone morphogenetic protein-2 and macrophage inhibitory cytokine-1 as mediators of the antiangiogenic activity of *N*-(4-hydroxyphenyl)retinamide. *Clin. Cancer Res.*, **2005**, *11*, 4610-4619.

[35] Formelli, F.; Cleris, L. Synthetic retinoid fenretinide is effective against a human ovarian carcinoma xenograft and potentiates cisplatin activity. *Cancer Res.*, **1993**, *53*, 5374-5376.

[36] Pienta, K. J.; Nguyen, N. M.; Lehr, J. E. Treatment of prostate cancer in the rat with the synthetic retinoid fenretinide. *Cancer Res.*, **1993**, *53*, 224-226.

[37] Chiesa, F.; Tradati, N.; Grigolato, R.; Boracchi, P.; Biganzoli, E.; Crose, N.; Cavadini, E.; Formelli, F.; Costa, L.; Giardini, R.; Zurrida, S.; Costa, A.; De Palo, G.; Veronesi, U. Randomized trial of fenretinide (4-HPR) to prevent recurrences, new localizations and carcinomas in patients operated on for oral leukoplakia: Long-term results. *Int. J. Cancer*, **2005**, *115*, 625-629.

[38] Bernard, B. A.; Bernardon, J. M.; Delescluse, C.; Martin, B.; Lenoir, M. C.; Maignan, J.; Charpentier, B.; Pilgrim, W. R.; Reichert, U.; Shroot, B. Identification of synthetic retinoids with selectivity for human nuclear retinoic acid receptor γ. *Biochem. Biophys. Res. Commun.*, **1992**, *186*, 977-983.

[39] Chao, W. R.; Hobbs, P. D.; Jong, L.; Zhang, X. K.; Zheng, Y.; Wu, Q.; Shroot, B.; Dawson, M. I. Effects of receptor class- and

subtype-selective retinoids and an apoptosis-inducing retinoid on the adherent growth of the NIH:OVCAR-3 ovarian cancer cell line in culture. *Cancer Lett.*, **1997**, *115*, 1-7.

[40] Shao, Z. M.; Dawson, M. I.; Li, X. S.; Rishi, A. K.; Sheikh, M. S.; Han, Q. X.; Ordonez, J. V.; Shroot, B.; Fontana, J. A. p53 independent G_0/G_1 arrest and apoptosis induced by a novel retinoid in human breast cancer cells. *Oncogene*, **1995**, *11*, 493-504.

[41] Fontana, J. A. Method for treating or preventing breast cancer or leukemia using 6-[3-(1-adamantyl)-4-hydroxyphenyl]-2-naphthalenecarboxylic acid. U.S. Patent 6,211,239, April 3, 2001.

[42] Li, X. S.; Rishi, A. K.; Shao, Z. M.; Dawson, M. I.; Jong, L.; Shroot, B.; Reichert, U.; Ordonez, J.; Fontana, J. A. Posttranscriptional regulation of $p21^{WAF1/CIP1}$ expression in human breast carcinoma cells. *Cancer Res.*, **1996**, *56*, 5055-5062.

[43] Hsu, C. K.; Rishi, A. K.; Li, X. S.; Dawson, M. I.; Reichert, U.; Shroot, B.; Fontana, J. A. Bcl-X_L expression and its downregulation by a novel retinoid in breast carcinoma cells. *Exp. Cell Res.*, **1997**, *232*, 17-24.

[44] Hsu, C. A.; Rishi, A. K.; Su-Li, X.; Gerald, T. M.; Dawson, M. I.; Schiffer, C.; Reichert, U.; Shroot, B.; Poirer, G. C.; Fontana, J. A. Retinoid induced apoptosis in leukemia cells through a retinoic acid nuclear receptor-independent pathway. *Blood*, **1997**, *89*, 4470-4479.

[45] Fontana, J. A.; Sun, R. J.; Rishi, A. K.; Dawson, M. I.; Ordonez, J. V.; Zhang, Y.; Tschang, S. H.; Bhalla, K.; Han, Z.; Wyche, J.; Poirer, G.; Sheikh, M. S.; Shroot, B.; Reichert, U. Overexpression of Bcl-2 or Bcl-X_L fails to inhibit apoptosis mediated by a novel retinoid. *Oncol. Res.*, **1998**, *10*, 313-324.

[46] Liang, J. Y.; Fontana, J. A.; Rao, J. N.; Ordonez, J. V.; Dawson, M. I.; Shroot, B.; Wilber, J. F.; Feng, P. Synthetic retinoid CD437 induces S-phase arrest and apoptosis in human prostate cancer cells LNCaP and PC-3. *Prostate*, **1999**, *38*, 228-236.

[47] Rishi, A. K.; Sun, R. J.; Gao, Y.; Hsu, C. K.; Gerald, T. M.; Sheikh, M. S.; Dawson, M. I.; Reichert, U.; Shroot, B.; Fornace, A. J., Jr.; Brewer, G.; Fontana, J. A. Post-transcriptional regulation of the DNA damage-inducible gadd45 gene in human breast carcinoma cells exposed to a novel retinoid CD437. *Nucleic Acids Res.*, **1999**, *27*, 3111-3119.

[48] Zhang, Y.; Huang, Y.; Rishi, A. K.; Sheikh, M. S.; Shroot, B.; Reichert, U.; Dawson, M.; Poirer, G.; Fontana, J. A. Activation of the p38 and JNK/SAPK mitogen-activated protein kinase pathways during apoptosis is mediated by a novel retinoid. *Exp. Cell Res.*, **1999**, *247*, 233-240.

[49] Farhana, L.; Dawson, M.; Rishi, A. K.; Zhang, Y.; Van Buren, E.; Trivedi, C.; Reichert, U.; Fang, G.; Kirschner, M. W.; Fontana, J. A. Cyclin B and E2F-1 expression in prostate carcinoma cells treated with the novel retinoid CD437 are regulated by the ubiquitin-mediated pathway. *Cancer Res.*, **2002**, *62*, 3842-3849.

[50] Rishi, A. K.; Zhang, L.; Boyanapalli, M.; Wali, A.; Mohammad, R. M.; Yu, Y.; Fontana, J. A.; Hatfield, J. S.; Dawson, M. I.; Majumdar, A. P.; Reichert, U. Identification and characterization of a cell cycle and apoptosis regulatory protein-1 as a novel mediator of apoptosis signaling by retinoid CD437. *J. Biol. Chem.*, **2003**, *278*, 33422-33435.

[51] Sakaue, M.; Adachi, H.; Dawson, M.; Jetten, A. M. Induction of Egr-1 expression by the retinoid AHPN in human lung carcinoma cells is dependent on activated ERK1/2. *Cell Death Differ.*, **2001**, *8*, 411-424.

[52] Sun, S. Y.; Yue, P.; Shroot, B.; Hong, W. K.; Lotan, R. Induction of apoptosis in human non-small cell lung carcinoma cells by the novel synthetic retinoid CD437. *J. Cell Physiol.*, **1997**, *173*, 279-284.

[53] Adachi, H.; Adams, A.; Hughes, F. M.; Zhang, J.; Cidlowski, J. A.; Jetten, A. M. Induction of apoptosis by the novel retinoid AHPN in human T-cell lymphoma cells involves caspase-dependent and independent pathways. *Cell Death Differ.*, **1998**, *5*, 973-983.

[54] Li, Y.; Lin, B.; Agadir, A.; Liu, R.; Dawson, M. I.; Reed, J. C.; Fontana, J. A.; Bost, F.; Hobbs, P. D.; Zheng, Y.; Chen, G. Q.; Shroot, B.; Mercola, D.; Zhang, X.-K. Molecular determinants of AHPN (CD437)-induced growth arrest and apoptosis in human lung cancer cell lines. *Mol. Cell Biol.*, **1998**, *18*, 4719-4731.

[55] Wu, S.; Zhang, D.; Donigan, A.; Dawson, M. I.; Soprano, D. R.; Soprano, K. J. Effects of conformationally restricted synthetic retinoids on ovarian tumor cell growth. *J. Cell Biochem.*, **1998**, *68*, 378-388.

[56] Sun, S. Y.; Kurie, J. M.; Yue, P.; Dawson, M. I.; Shroot, B.; Chandraratna, R. A. S.; Hong, W. K.; Lotan, R. Differential responses of normal, premalignant, and malignant human bronchial epithelial cells to receptor-selective retinoids. *Clin. Cancer Res.*, **1999**, *5*, 431-437.

[57] Meister, B.; Fink, F. M.; Hittmair, A.; Marth, C.; Widschwendter, M. Antiproliferative activity and apoptosis induced by retinoic acid receptor-γ selectively binding retinoids in neuroblastoma. *Anticancer Res.*, **1998**, *18*, 1777-1786.

[58] Gianni, M.; de Thé, H. In acute promyelocytic leukemia NB4 cells, the synthetic retinoid CD437 induces contemporaneously apoptosis, a caspase-3-mediated degradation of PML/RARα protein and the PML retargeting on PML-nuclear bodies. *Leukemia*, **1999**, *13*, 739-749.

[59] Gonda, K.; Tsuchiya, H.; Sakabe, T.; Akechi, Y.; Ikeda, R.; Nishio, R.; Terabayashi, K.; Ishii, K.; Matsumi, Y.; Ashla, A. A.; Okamoto, H.; Takubo, K.; Matsuoka, S.; Watanabe, Y.; Hoshikawa, Y.; Kurimasa, A.; Shiota, G. Synthetic retinoid CD437 induces mitochondria-mediated apoptosis in hepatocellular carcinoma cells. *Biochem. Biophys. Res. Commun.*, **2008**, *370*, 629-633.

[60] Zhao, X.; Demary, K.; Wong, L.; Vaziri, C.; McKenzie, A. B.; Eberlein, T. J.; Spanjaard, R. A. Retinoic acid receptor-independent mechanism of apoptosis of melanoma cells by the retinoid CD437 (AHPN). *Cell Death Differ.*, **2001**, *8*, 878-886.

[61] Sun, S. Y.; Yue, P.; Chen, X.; Hong, W. K.; Lotan, R. The synthetic retinoid CD437 selectively induces apoptosis in human lung cancer cells while sparing normal human lung epithelial cells. *Cancer Res.*, **2002**, *62*, 2430-2436.

[62] Sun, S. Y.; Yue, P.; Chandraratna, R. A. S.; Tesfaigzi, Y.; Hong, W.-K.; Lotan, R. Dual mechanisms of action of the retinoid CD437: Nuclear retinoic acid receptor-mediated suppression of squamous differentiation and receptor-independent induction of apoptosis in UMSCC22B human head and neck squamous cell carcinoma cells. *Mol. Pharmacol.*, **2000**, *58*, 508-514.

[63] Sun, S. Y.; Yue, P.; Mao, L.; Dawson, M. I.; Shroot, B.; Lamph, W. W.; Heyman, R. A.; Chandraratna, R. A. S.; Shudo, K.; Hong, W. K.; Lotan, R. Identification of receptor-selective retinoids that are potent inhibitors of the growth of human head and neck squamous cell carcinoma cells. *Clin. Cancer Res.*, **2000**, *6*, 1563-1573.

[64] Zang, Y.; Beard, R. L.; Chandraratna, R. A. S.; Kang, J. X. Evidence of a lysosomal pathway for apoptosis induced by the synthetic retinoid CD437 in human leukemia HL-60 cells. *Cell Death Differ.*, **2001**, *8*, 477-485.

[65] Pfahl, M.; Piedrafita, F. J. Retinoid targets for apoptosis induction. *Oncogene*, **2003**, *22*, 9058-9062.

[66] Lu, X. P.; Fanjul, A.; Picard, N.; Pfahl, M.; Rungta, D.; Nared-Hood, K.; Carter, B.; Piedrafita, J.; Tang, S.; Fabbrizio, E. Novel retinoid-related molecules as apoptosis inducers and effective inhibitors of human lung cancer cells *in vivo*. *Nat. Med.*, **1997**, *3*, 686-690.

[67] Pfahl, M. Retinoid related molecules: New promises against lung and breast cancer. *Expert Opin. Investig. Drugs* **1998**, *7*, 601-606.

[68] Yarovoi, S. V.; Lu, X. P.; Picard, N.; Rungta, D.; Rideout, D.; Pfahl, M. Selective activation of an apoptotic retinoid precursor in macrophage cell lines. *J. Biol. Chem.*, **1998**, *273*, 20852-20859.

[69] Fanjul, A. N.; Piedrafita, F. J.; Al-Shamma, H.; Pfahl, M. Apoptosis induction and potent antiestrogen receptor-negative breast cancer activity *in vivo* by a retinoid antagonist. *Cancer Res.*, **1998**, *58*, 4607-4610.

[70] Lu, X. P.; Fanjul, A.; Picard, N.; Shroot, B.; Pfahl, M. A selective retinoid with high activity against an androgen-resistant prostate cancer cell type. *Int. J. Cancer*, **1999**, *80*, 272-278.

[71] Cincinelli, R.; Dallavalle, S.; Merlini, L.; Penco, S.; Pisano, C.; Carminati, P.; Giannini, G.; Vesci, L.; Gaetano, C.; Illy, B.; Zuco, V.; Supino, R.; Zunino, F. A novel atypical retinoid endowed with proapoptotic and antitumor activity. *J. Med. Chem.*, **2003**, *46*, 909-912.

[72] Di Francesco, A. M.; Meco, D.; Torella, A. R.; Barone, G.; D'Incalci, M.; Pisano, C.; Carminati, P.; Riccardi, R. The novel atypical retinoid ST1926 is active in ATRA resistant neuroblastoma cells acting by a different mechanism. *Biochem. Pharmacol.*, **2007**, *73*, 643-655.

[73] Zuco, V.; Zanchi, C.; Lanzi, C.; Beretta, G. L.; Supino, R.; Pisano, C.; Barbarino, M.; Zanier, R.; Bucci, F.; Aulicino, C.; Carminati, P.; Zunino, F. Development of resistance to the atypical retinoid, ST1926, in the lung carcinoma cell line H460 is associated with reduced formation of DNA strand breaks and a defective DNA damage response. *Neoplasia*, **2005**, *7*, 667-677.

[74] Garattini, E.; Gianni, M.; Terao, M. Retinoid related molecules an emerging class of apoptotic agents with promising therapeutic potential in oncology: Pharmacological activity and mechanisms of action. *Curr. Pharm. Des.*, **2004**, *10*, 433-448.

[75] Garattini, E.; Parrella, E.; Diomede, L.; Gianni, M.; Kalac, Y.; Merlini, L.; Simoni, D.; Zanier, R.; Ferrara, F. F.; Chiarucci, I.; Carminati, P.; Terao, M.; Pisano, C. ST1926, a novel and orally active retinoid-related molecule inducing apoptosis in myeloid leukemia cells: Modulation of intracellular calcium homeostasis. *Blood*, **2004**, *103*, 194-207.

[76] Parrella, E.; Gianni, M.; Fratelli, M.; Barzago, M. M.; Raska, I., Jr.; Diomede, L.; Kurosaki, M.; Pisano, C.; Carminati, P.; Merlini, L.; Dallavalle, S.; Tavecchio, M.; Rochette-Egly, C.; Terao, M.; Garattini, E. Antitumor activity of the retinoid-related molecules (*E*)-3-(4´-hydroxy-3´-adamantylbiphenyl-4-yl)acrylic acid (ST1926) and 6-[3-(1-adamantyl)-4-hydroxyphenyl]-2-naphthalenecarboxylic acid (CD437) in F9 teratocarcinoma: Role of retinoic acid receptor γ and retinoid-independent pathways. *Mol. Pharmacol.*, **2006**, *70*, 909-924.

[77] Valli, C.; Paroni, G.; Di Francesco, A. M.; Riccardi, R.; Tavecchio, M.; Erba, E.; Boldetti, A.; Gianni, M.; Fratelli, M.; Pisano, C.; Merlini, L.; Antoccia, A.; Cenciarelli, C.; Terao, M.; Garattini, E. Atypical retinoids ST1926 and CD437 are S-phase-specific agents causing DNA double-strand breaks: Significance for the cytotoxic and antiproliferative activity. *Mol. Cancer Ther.*, **2008**, *7*, 2941-2954.

[78] Pisano, C.; Vesci, L.; Fodera, R.; Ferrara, F. F.; Rossi, C.; De Cesare, M.; Zuco, V.; Pratesi, G.; Supino, R.; Zunino, F. Antitumor activity of the combination of synthetic retinoid ST1926 and cisplatin in ovarian carcinoma models. *Ann. Oncol.*, **2007**, *18*, 1500-1505.

[79] Zuco, V.; Benedetti, V.; De Cesare, M.; Zunino, F. Sensitization of ovarian carcinoma cells to the atypical retinoid ST1926 by the histone deacetylase inhibitor, RC307: Enhanced DNA damage response. *Int. J. Cancer*, **2010**, *126*, 1246-1255.

[80] Sala, F.; Zucchetti, M.; Bagnati, R.; D'Incalci, M.; Pace, S.; Capocasa, F.; Marangon, E. Development and validation of a liquid chromatography-tandem mass spectrometry method for the determination of ST1926, a novel oral antitumor agent, adamantyl retinoid derivative, in plasma of patients in a phase I study. *J. Chromatogr. B, Analyt. Technol. Biomed. Life Sci.*, **2009**, *877*, 3118-3126.

[81] Fontana, J. A.; Dawson, M. I.; Leid, M.; Rishi, A. K.; Zhang, Y.; Hsu, C. A.; Lu, J. S.; Peterson, V. J.; Jong, L.; Hobbs, P.; Chao, W. R.; Shroot, B.; Reichert, U. Identification of a unique binding protein specific for a novel retinoid inducing cellular apoptosis. *Int. J. Cancer*, **2000**, *86*, 474-479.

[82] Farhana, L.; Dawson, M. I.; Leid, M.; Wang, L.; Moore, D. D.; Liu, G.; Xia, Z.; Fontana, J. A. Adamantyl-substituted retinoid-related molecules bind small heterodimer partner and modulate the Sin3A repressor. *Cancer Res.*, **2007**, *67*, 318-325.

[83] Farhana, L.; Dawson, M. I.; Dannenberg, J. H.; Xu, L.; Fontana, J. A. SHP and Sin3A expression are essential for adamantyl-substituted retinoid-related molecule-mediated nuclear factor-κB activation, c-Fos/c-Jun expression, and cellular apoptosis. *Mol. Cancer Ther.*, **2009**, *8*, 1625-1635.

[84] Dawson, M. I.; Hobbs, P. D.; Peterson, V. J.; Leid, M.; Lange, C. W.; Feng, K. C.; Chen, G.; Gu, J.; Li, H.; Kolluri, S. K.; Zhang, X.; Zhang, Y.; Fontana, J. A. Apoptosis induction in cancer cells by a novel analogue of 6-[3-(1-adamantyl)-4-hydroxyphenyl]-2-naphthalenecarboxylic acid lacking retinoid receptor transcriptional activation activity. *Cancer Res.*, **2001**, *61*, 4723-4730.

[85] Zhang, Y.; Dawson M. I.; Mohammad R.; Rishi A. K.; Farhana L.; Feng K. C.; Leid M.; Peterson V.; Zhang X.-K.; Edelstein M.; Eilander D.; Biggar S.; Wall N.; Reichert U.; Fontana J. A. Induction of apoptosis of human B-CLL and ALL cells by a novel retinoid and its nonretinoidal analog. *Blood*, **2002**, 100, 2917-2925.

[86] Zhang, Y.; Dawson, M. I.; Ning, Y.; Polin, L.; Parchment, R. E.; Corbett, T.; Mohamed, A. N.; Feng, K.-C.; Farhana, L.; Rishi, A. K.; Hogge, D.; Leid, M.; Peterson, V. J.; Zhang, X.-K.; Mohammad, R.; Lu, J. S.; Willman, C.; VanBuren, E.; Biggar, S.; Edelstein, M.; Eilender, D.; Fontana, J. A. Induction of apoptosis in retinoid-refractory acute myelogenous leukemia by a novel AHPN analog. *Blood*, **2003**, *102*, 3743-3752.

[87] Farhana, L.; Dawson, M. I.; Huang, Y.; Zhang, Y.; Rishi, A. K.; Reddy, K. B.; Freeman, R. S.; Fontana, J. A. Apoptosis signaling by the novel compound 3-Cl-AHPC involves increased EGFR proteolysis and accompanying decreased phosphatidylinositol 3-kinase and AKT kinase activities. *Oncogene*, **2004**, *23*, 1874-1884.

[88] Dawson, M. I.; Fontana, J.A.; Zhang, X-.K.; Leid, M., Jong, L., Hobbs, P.D. Induction of apoptosis in cancer cells. U.S. Patent 7,053,071, May 30, 2006.

[89] Pisano, C.; Vesci, L. Use of adamantyl methoxydiphenylpropenoic acid for the treatment of acne. U.S. Patent 7,635,719, December 22, 2009.

[90] Dawson, M. I.; Xia, Z.; Liu, G.; Ye, M.; Fontana, J. A.; Farhana, L.; Patel, B. B.; Arumugarajah, S.; Bhuiyan, M.; Zhang, X.-K.; Han, Y. H.; Stallcup, W. B.; Fukushi, J.; Mustelin, T.; Tautz, L.; Su, Y.; Harris, D. L.; Waleh, N.; Hobbs, P. D.; Jong, L.; Chao, W.-R.; Schiff, L. J.; Sani, B. P. An adamantyl-substituted retinoid-derived molecule that inhibits cancer cell growth and angiogenesis by inducing apoptosis and binds to small heterodimer partner nuclear receptor: Effects of modifying its carboxylate group on apoptosis, proliferation, and protein-tyrosine phosphatase activity. *J. Med. Chem.*, **2007**, *50*, 2622-2639.

[91] Dawson, M. I.; Xia, Z., Jiang, T.; Ye, M.; Fontana, J. A.; Farhana, L.; Patel, B.; Xue, L. P.; Bhuiyan, M.; Pellicciari, R.; Macchiarulo, A.; Nuti, R.; Zhang, X.-K.; Han, Y. H.; Tautz, L.; Hobbs, P. D.; Jong, L.; Waleh, N.; Chao, W.-R.; Feng, G. S.; Pang, Y.; Su, Y. Adamantyl-substituted retinoid-derived molecules that interact with the orphan nuclear receptor small heterodimer partner: Effects of replacing the 1-adamantyl or hydroxyl group on inhibition of cancer cell growth, induction of cancer cell apoptosis, and inhibition of SRC homology 2 domain-containing protein tyrosine phosphatase-2 activity. *J. Med. Chem.*, **2008**, *51*, 5650-5662.

[92] Charpentier, B.; Bernardon, J. M.; Eustache, J.; Millois, C.; Martin, B.; Michel, S.; Shroot, B. Synthesis, structure–affinity relationships, and biological activities of ligands binding to retinoic acid receptor subtypes. *J. Med. Chem.*, **1995**, *38*, 4993-5006.

[93] Pérez-Rodríguez, S.; Ortiz, M. A.; Pereira, R.; Rodriguez-Barrios, F.; de Lera, A. R.; Piedrafita, F. J. Highly twisted adamantyl arotinoids: Synthesis, antiproliferative effects and RXR transactivation profiles. *Eur. J. Med. Chem.*, **2009**, *44*, 2434-2446.

[94] Lorenzo, P.; Alvarez, R.; Ortiz, M. A.; Alvarez, S.; Piedrafita, F. J.; de Lera, A. R. Inhibition of IκB kinase-β and anticancer activities of novel chalcone adamantyl arotinoids. *J. Med. Chem.*, **2008**, *51*, 5431-5440.

[95] Macchiarulo, A.; Rizzo, G.; Costantino, G.; Fiorucci, S.; Pellicciari, R. Unveiling hidden features of orphan nuclear receptors: The case of the small heterodimer partner (SHP). *J. Mol. Graph Model.*, **2006**, *24*, 362-372.

[96] Evans, R. M.; Ong, E.; Segui, P.S.; Thompson, C.C.; Umesomo, K.; Giguere, V. Retinoic acid receptor method. U.S. Patent 4,981,784, January 1, 1991.

[97] Evans, R. M.; Heyman, R.A.; Berger, C.S.; Stein, R.B. Use of selective ligands for treatment of disease states responsive to steroid or steroid-like hormones. U.S. Patent 6,096,787, August 1, 2000.

[98] Dawson, M. I.; Harris, D. L.; Liu, G.; Hobbs, P. D.; Lange, C. W.; Jong, L.; Bruey-Sedano, N.; James, S. Y.; Zhang, X.-K.; Peterson, V. J.; Leid, M.; Farhana, L.; Rishi, A. K.; Fontana, J. A. Antagonist analogue of 6-[3´-(1-adamantyl)-4´-hydroxyphenyl]-2-naphthalenecarboxylic acid (AHPN) family of apoptosis inducers that effectively blocks AHPN-induced apoptosis but not cell-cycle arrest. *J. Med. Chem.*, **2004**, *47*, 3518-3536.

[99] Cincinelli, R.; Dallavalle, S.; Nannei, R.; Merlini, L.; Penco, S.; Giannini, G.; Pisano, C.; Vesci, L.; Ferrara, F. F.; Zuco, V.; Zanchi, C.; Zunino, F. Synthesis and structure-activity relationships of new antiproliferative and proapoptotic retinoid-related biphenyl-4-yl-acrylic acids. *Bioorg. Med. Chem.*, **2007**, *15*, 4863-4875.

[100] Kagechika, H.; Kawachi, E.; Hashimoto, Y.; Shudo, K. Retinobenzoic acids. 2. Structure-activity relationships of chalcone-4-carboxylic acids and flavone-4'-carboxylic acids. *J. Med. Chem.*, **1989**, *32*, 834-840.

[101] Lopez-Hernandez, F. J.; Ortiz, M. A.; Bayon, Y.; Piedrafita, F. J. Z-FA-fmk inhibits effector caspases but not initiator caspases 8 and 10, and demonstrates that novel anticancer retinoid-related molecules induce apoptosis *via* the intrinsic pathway. *Mol. Cancer Ther.*, **2003**, *2*, 255-263.

[102] Adachi, H.; Preston, G.; Harvat, B.; Dawson, M. I.; Jetten, A. M. Inhibition of cell proliferation and induction of apoptosis by the retinoid AHPN in human lung carcinoma cells. *Am. J. Respir. Cell. Mol. Biol.*, **1998**, *18*, 323-333.

[103] Holmes, W. F.; Dawson, M. I.; Soprano, R. D.; Soprano, K. J. Induction of apoptosis in ovarian carcinoma cells by AHPN/CD437 is mediated by retinoic acid receptors. *J. Cell Physiol.*, **2000**, *185*, 61-67.

[104] Hsu, S. L.; Yin, S. C.; Liu, M. C.; Reichert, U.; Ho, W. L. Involvement of cyclin-dependent kinase activities in CD437-induced apoptosis. *Exp. Cell Res.*, **1999**, *252*, 332-341.

[105] Costa, S. L.; Paillaud, E.; Fages, C.; Rochette-Egly, C.; Plassat, J. L.; Jouault, H.; Perzelova, A.; Tardy, M. Effects of a novel synthetic retinoid on malignant glioma *in vitro*: Inhibition of cell proliferation, induction of apoptosis and differentiation. *Eur. J. Cancer*, **2001**, *37*, 520-530.

[106] Zhang, Y.; Rishi, A. K.; Dawson, M. I.; Tschang, R.; Farhana, L.; Boyanapalli, M.; Reichert, U.; Shroot, B.; Van Buren, E. C.; Fontana, J. A. S-phase arrest and apoptosis induced in normal mammary epithelial cells by a novel retinoid. *Cancer Res.*, **2000**, *60*, 2025-2032.

[107] Nicholson, D. W.; Ali, A.; Thornberry, N. A.; Vaillancourt, J. P.; Ding, C. K.; Gallant, M.; Gareau, Y.; Griffin, P. R.; Labelle, M.; Lazebnik, Y. A.; Munday, N. A.; Raju, S. M.; Smulson, M. E.; Yamin, T.-T.; Yu, V. L.; Miller, D. K. Identification and inhibition of the ICE/CED-3 protease necessary for mammalian apoptosis. *Nature*, **1995**, *376*, 37-43.

[108] Fernandes-Alnemri, T.; Litwack, G.; Alnemri, E. S. CPP32, a novel human apoptotic protein with homology to *Caenorhabditis elegans* cell death protein Ced-3 and mammalian interleukin-1β-converting enzyme. *J. Biol. Chem.*, **1994**, *269*, 30761-30764.

[109] Kumar, S.; Lavin, M. F. The ICE family of cysteine proteases as effectors of cell death. *Cell Death Differ.*, **1996**, *3*, 255-267.

[110] Ortiz, M. A.; Lopez-Hernandez, F. J.; Bayon, Y.; Pfahl, M.; Piedrafita, F. J. Retinoid-related molecules induce cytochrome *c* release and apoptosis through activation of c-Jun NH_2-terminal kinase/p38 mitogen-activated protein kinases. *Cancer Res.*, **2001**, *61*, 8504-8512.

[111] Holmes, W. F.; Soprano, D. R.; Soprano, K. J. Early events in the induction of apoptosis in ovarian carcinoma cells by CD437: Activation of the p38 MAP kinase signal pathway. *Oncogene*, **2003**, *22*, 6377-6386.

[112] Boisvieux-Ulrich, E.; Sourdeval, M.; Marano, F. CD437, a synthetic retinoid, induces apoptosis in human respiratory epithelial cells *via* caspase-independent mitochondrial and caspase-8-dependent pathways both up-regulated by JNK signaling pathway. *Exp. Cell Res.*, **2005**, *307*, 76-90.

[113] Lin, B.; Kolluri, S. K.; Lin, F.; Liu, W.; Han, Y. H.; Cao, X.; Dawson, M. I.; Reed, J. C.; Zhang, X.-K. Conversion of Bcl-2 from protector to killer by interaction with nuclear orphan receptor Nur77/TR3. *Cell*, **2004**, *116*, 527-540.

[114] Liang, B.; Song, X.; Liu, G.; Li, R.; Xie, J.; Xiao, L.; Du, M.; Zhang, Q.; Xu, X.; Gan, X.; Huang, D. Involvement of TR3/Nur77 translocation to the endoplasmic reticulum in ER stress-induced apoptosis. *Exp. Cell Res.*, **2007**, *313*, 2833-2844.

[115] Beg, A. A.; Baltimore, D. An essential role for NF-κB in preventing TNF-α-induced cell death. *Science*, **1996**, *274*, 782-784.

[116] Beg, A. A.; Sha, W. C.; Bronson, R. T.; Ghosh, S.; Baltimore, D. Embryonic lethality and liver degeneration in mice lacking the RelA component of NF-κB. *Nature*, **1995**, *376*, 167-170.

[117] Van Antwerp, D. J.; Martin, S. J.; Kafri, T.; Green, D. R.; Verma, I. M. Suppression of TNF-α-induced apoptosis by NF-κB. *Science*, **1996**, *274*, 787-789.

[118] Turco, M. C.; Romano, M. F.; Petrella, A.; Bisogni, R.; Tassone, P.; Venuta, S. NF-κB/Rel-mediated regulation of apoptosis in hematologic malignancies and normal hematopoietic progenitors. *Leukemia*, **2004**, *18*, 11-17.

[119] Abbadie, C.; Kabrun, N.; Bouali, F.; Smardova, J.; Stéhelin, D.; Vandenbunder, B.; Enrietto, P. J. High levels of *c-rel* expression are associated with programmed cell death in the developing avian embryo and in bone marrow cells *in vitro*. *Cell*, **1993**, *75*, 899-912.

[120] Kitajima, I.; Soejima, Y.; Takasaki, I.; Beppu, H.; Tokioka, T.; Maruyama, I. Ceramide-induced nuclear translocation of NF-κB is a potential mediator of the apoptotic response to TNF-α in murine clonal osteoblasts. *Bone*, **1996**, *19*, 263-270.

[121] Hunot, S.; Brugg, B.; Ricard, D.; Michel, P. P.; Muriel, M. P.; Ruberg, M.; Faucheux, B. A.; Agid, Y.; Hirsch, E. C. Nuclear translocation of NF-κB is increased in dopaminergic neurons of patients with Parkinson disease. *Proc. Natl. Acad. Sci. U.S.A.*, **1997**, *94*, 7531-7536.

[122] Panet, H.; Barzilai, A.; Daily, D.; Melamed, E.; Offen, D. Activation of nuclear transcription factor kappa B (NF-κB) is essential for dopamine-induced apoptosis in PC12 cells. *J. Neurochem.*, **2001**, *77*, 391-398.

[123] Muller, I.; Pfister, S. M.; Grohs, U.; Zweigner, J.; Handgretinger, R.; Niethammer, D.; Bruchelt, G. Receptor activator of nuclear factor κB ligand plays a nonredundant role in doxorubicin-induced apoptosis. *Cancer Res.*, **2003**, *63*, 1772-1775.

[124] Huang, Y.; Fang, Y.; Wu, J.; Dziadyk, J. M.; Zhu, X.; Sui, M.; Fan, W. Regulation of *Vinca* alkaloid-induced apoptosis by NF-κB/IκB pathway in human tumor cells. *Mol. Cancer Ther.*, **2004**, *3*, 271-277.

[125] Farhana, L.; Dawson, M. I.; Fontana, J. A. Apoptosis induction by a novel retinoid-related molecule requires nuclear factor-κB activation. *Cancer Res.*, **2005**, *65*, 4909-4917.

[126] Jin, F.; Liu, X.; Zhou, Z.; Yue, P.; Lotan, R.; Khuri, F. R.; Chung, L. W.; Sun, S. Y. Activation of nuclear factor-κB contributes to induction of death receptors and apoptosis by the synthetic retinoid CD437 in DU145 human prostate cancer cells. *Cancer Res.*, **2005**, *65*, 6354-6363.

[127] Schadendorf, D.; Kern, M. A.; Artuc, M.; Pahl, H. L.; Rosenbach, T.; Fichtner, I.; Nurnberg, W.; Stuting, S.; von Stebut, E.; Worm, M.; Makki, A.; Jurgovsky, K.; Kolde, G.; Henz, B. M. Treatment of melanoma cells with the synthetic retinoid CD437 induces apoptosis *via* activation of AP-1 *in vitro*, and causes growth inhibition in xenografts *in vivo*. *J. Cell Biol.*, **1996**, *135*, 1889-1898.

[128] Langdon, S. P.; Rabiasz, G. J.; Ritchie, A. A.; Reichert, U.; Buchan, P.; Miller, W. R.; Smyth, J. F. Growth-inhibitory effects of the synthetic retinoid CD437 against ovarian carcinoma models *in vitro* and *in vivo*. *Cancer Chemother. Pharmacol.*, **1998**, *42*, 429-432.

[129] Liu, T. J.; Koul, D.; LaFortune, T.; Tiao, N.; Shen, R. J.; Maira, S. M.; Garcia-Echevrria, C.; Yung, W. K. NVP-BEZ235, a novel dual phosphatidylinositol 3-kinase/mammalian target of rapamycin inhibitor, elicits multifaceted antitumor activities in human gliomas. *Mol. Cancer Ther.*, **2009**, *8*, 2204-2210.

[130] Liu, S.; Brown, C. W.; Berlin, K. D.; Dhar, A.; Guruswamy, S.; Brown, D.; Gardner, G. J.; Birrer, M. J.; Benbrook, D. M. Synthesis of flexible sulfur-containing heteroarotinoids that induce apoptosis and reactive oxygen species with discrimination between malignant and benign cells. *J. Med. Chem.*, **2004**, *47*, 999-1007.

[131] Sousa, M. O.; Miranda, T. L.; Costa, E. B.; Bittar, E. R.; Santoro, M. M.; Figueiredo, A. F. Linear competitive inhibition of human tissue kallikrein by 4-aminobenzamidine and benzamidine and linear mixed inhibition by 4-nitroaniline and aniline. *Braz. J. Med. Biol. Res.*, **2001**, *34*, 35-44.

[132] Assmann, N.; Emmrich, M.; Kampf, G.; Kaiser, M. Genotoxic activity of important nitrobenzenes and nitroanilines in the Ames test and their structure-activity relationship. *Mutat. Res.*, **1997**, *395*, 139-144.

[133] Nair, R. S.; Auletta, C. S.; Schroeder, R. E.; Johannsen, F. R. Chronic toxicity, oncogenic potential, and reproductive toxicity of *p*-nitroaniline in rats. *Fundam. Appl. Toxicol.*, **1990**, *15*, 607-621.

[134] Spruce, L. W.; Gale, J. B.; Berlin, K. D.; Verma, A. K.; Breitman, T. R.; Ji, X. H.; van der Helm, D. Novel heteroarotinoids: Synthesis and biological activity. *J. Med. Chem.*, **1991**, *34*, 430-439.

[135] Zacheis, D.; Dhar, A.; Lu, S.; Madler, M. M.; Klucik, J.; Brown, C. W.; Liu, S.; Clement, F.; Subramanian, S.; Weerasekare, G. M.; Berlin, K. D.; Gold, M. A.; Houck, J. R., Jr.; Fountain, K. R.; Benbrook, D. M. Heteroarotinoids inhibit head and neck cancer cell lines *in vitro* and *in vivo* through both RAR and RXR retinoic acid receptors. *J. Med. Chem.*, **1999**, *42*, 4434-4445.

[136] Dhar, A.; Liu, S.; Klucik, J.; Berlin, K. D.; Madler, M. M.; Lu, S.; Ivey, R. T.; Zacheis, D.; Brown, C. W.; Nelson, E. C.; Birckbichler, P. J.; Benbrook, D. M. Synthesis, structure-activity relationships, and RARγ-ligand interactions of nitrogen heteroarotinoids. *J. Med. Chem.*, **1999**, *42*, 3602-3614.

[137] Dawson, M. I.; Hobbs, P. D.; Derdzinski, K.; Chan, R. L.; Gruber, J.; Chao, W. R.; Smith, S.; Thies, R. W.; Schiff, L. J. Conformationally restricted retinoids. *J. Med. Chem.*, **1984**, *27*, 1516-1531.

[138] Waugh, K. M.; Berlin, K. D.; Ford, W. T.; Holt, E. M.; Carrol, J. P.; Schomber, P. R.; Thompson, M. D.; Schiff, L. J. Synthesis and characterization of selected heteroarotinoids. Pharmacological activity as assessed in vitamin A deficient hamster tracheal organ cultures. Single-crystal X-ray diffraction analysis of 4,4-dimethylthiochroman-6-yl methyl ketone 1,1-dioxide and ethyl (*E*)-*p*-[2-(4,4-dimethylthiochroman-6-yl)propenyl]benzoate. *J. Med. Chem.*, **1985**, *28*, 116-124.

[139] Benbrook, D. M.; Kamelle, S. A.; Guruswamy, S. B.; Lightfoot, S. A.; Rutledge, T. L.; Gould, N. S.; Hannafon, B. N.; Dunn, S. T.; Berlin, K. D. Flexible heteroarotinoids (Flex-Hets) exhibit improved therapeutic ratios as anticancer agents over retinoic acid receptor agonists. *Invest. New Drugs*, **2005**, *23*, 417-428.

[140] Chun, K.-H.; Benbrook, D. M.; Berlin, K. D.; Hong, W. K.; Lotan, R. The synthetic heteroarotinoid SHetA2 induces apoptosis in squamous carcinoma cells through a receptor-independent and mitochondria-dependent pathway. *Cancer Res.*, **2003**, *63*, 3826-3832.

[141] Lin, Y. D.; Chen, S.; Yue, P.; Zou, W.; Benbrook, D. M.; Liu, S.; Le, T. C.; Berlin, K. D.; Khuri, F. R.; Sun, S. Y. CAAT/enhancer binding protein homologous protein-dependent death receptor 5 induction is a major component of SHetA2-induced apoptosis in lung cancer cells. *Cancer Res.*, **2008**, *68*, 5335-5344.

[142] Myers, T.; Chengedza, S.; Lightfoot, S.; Pan, Y.; Dedmond, D.; Cole, L.; Tang, Y.; Benbrook, D. M. Flexible heteroarotinoid (Flex-Het) SHetA2 inhibits angiogenesis *in vitro* and *in vivo*. *Invest. New Drugs*, **2009**, *27*, 304-318.

[143] Zhang, Y.; Hua, Y.; Benbrook, D. M.; Covey, J. M.; Dai, G.; Liu, Z.; Chan, K. K. High performance liquid chromatographic analysis and preclinical pharmacokinetics of the heteroarotinoid antitumor agent, SHetA2. *Cancer Chemother. Pharmacol.*, **2006**, *58*, 561-569.

[144] Liu, T.; Hannafon, B.; Gill, L.; Kelly, W.; Benbrook, D. Flex-Hets differentially induce apoptosis in cancer over normal cells by directly targeting mitochondria. *Mol. Cancer Ther.*, **2007**, *6*, 1814-1822.

[145] Bhatnagar, R.; Abou-Issa, H.; Curley, R. W., Jr.; Koolemans-Beynen, A.; Moeschberger, M. L.; Webb, T. E. Growth suppression of human breast carcinoma cells in culture by *N*-(4-hydroxyphenyl)retinamide and its glucuronide and through synergism with glucarate. *Biochem. Pharmacol.*, **1991**, *41*, 1471-1477.

[146] Abou-Issa, H.; Curley, R. W., Jr.; Panigot, M. J.; Tanagho, S. N.; Sidhu, B. S.; Alshafie, G. A. Chemotherapeutic evaluation of *N*-(4-hydroxyphenyl) retinamide-*O*-glucuronide in the rat mammary tumor model. *Anticancer Res.*, **1997**, *17*, 3335-3339.

[147] Liu, T. J.; Koul, D.; LaFortune, T.; Tiao, N.; Shen, R. J.; Maira, S. M.; Garcia-Echevrria, C.; Yung, W. K. NVP-BEZ235, a novel dual phosphatidylinositol 3-kinase/mammalian target of rapamycin inhibitor, elicits multifaceted antitumor activities in human gliomas. *Mol. Cancer Ther.*, **2009**, *8*, 2204-2210.

[148] Le, T. C.; Berlin, K. D.; Benson, S. D.; Eastman, M. A.; Bell-Eunice, G.; Nelson, A. C.; Benbrook, D. M. Heteroarotinoids with anticancer activity against ovarian cancer cells. *Open Med. Chem. J.*, **2007**, *1*, 11-23.

Received: January 05, 2010 Revised: March 12, 2010 Accepted: March 14, 2010